Delft University of Technology
Master of Science Thesis in Embedded Systems

Passive Visible Light Communication using low-cost colour filters

Jasper Jonk

TU Delft Delft University of Technology

Passive Visible Light Communication using low-cost colour filters

Master of Science Thesis in Embedded Systems

Networked Systems Group
Faculty of Electrical Engineering, Mathematics and Computer Science
Delft University of Technology
Van Mourik Broekmanweg 6, 2628 XE Delft, The Netherlands

Jasper Jonk
j.jonk@student.tudelft.nl
jasper.jonk@outlook.com

01-05-2023

Author
Jasper Jonk (j.jonk@student.tudelft.nl)
(jasper.jonk@outlook.com)

Title
Passive Visible Light Communication using low-cost colour filters

MSc Presentation Date
09-05-2023

Graduation Committee

Marco Zuniga	Delft University of Technology
Johan Pouwelse	Delft University of Technology

Abstract

Due to trends such as the Internet of Things, there has been a growing number of devices that use wireless technologies for communication. This increase leads to bandwidth limitations that forced researchers to explore other types of wireless communication. One of these alternatives is Visible Light Communication (VLC).

VLC encodes data by rapidly changing the intensity of a source emitting light in the visible spectrum. One branch of VLC is Passive VLC. Passive VLC uses ambient light, such as sunlight or ceiling lamps, as a source. An advantage of this approach is the drastically reduced power consumption. Since the light is already present, no energy has to be used to power a source. However, a flaw of Passive VLC is the lower throughput due to limitations in the available modulation devices.

This thesis aims to mitigate the limited throughput by creating separate independent bands that can simultaneously transmit data. Taking advantage of the relatively wide visible light spectrum, the use of colour filters will be explored to divide the spectrum into distinct bands where independent data can be transmitted. To keep it as accessible as possible, there is a focus on low-cost filters, reducing computational complexity and real-time communication. A characterisation of low-cost colour filters is presented as well as a channel estimation algorithm to mitigate the shortcomings of inexpensive filters. To reduce the computational overhead, an encoding algorithm is presented that drastically reduces the computation needed to decode data.

Ultimately, we provide a physical platform that achieves multi-channel passive VLC by exploiting cost-effective colour filters. The platform allows for simple expansion to greater numbers of channels as well as real-time communication due to the ability to adjust to the surrounding conditions.

Contents

Chapter 1

Introduction

Wireless data transmission is ubiquitous and often goes unnoticed by humans. However, numerous everyday items rely on wireless data to function, such as mobile phones or conventional radios. Radios tune into a set frequency in the Radio Frequency (RF) spectrum to demodulate data. This technology stems from the last decade [7] but it is still relevant today as it defines the basic principle for wireless communication. Since then, there has been a significant development in the field of wireless RF communication. Technologies such as WiFi, LoRa, Bluetooth and GSM are all examples of recent developments. The number of wireless communication devices has rapidly grown in recent years, with trends such as the Internet of Things (IoT) driving this growth. All devices need a certain band in the RF spectrum to communicate. However, with the increasing number of devices, this bandwidth is harder to come by. The scarcity of available bandwidth in the RF spectrum has become a significant challenge for wireless communication. Researchers have sought out new domains to expand the available bandwidth and the visible light spectrum is considered to be one of the promising fields.

The visible light spectrum and the RF spectrum both capture a part of the electromagnetic spectrum. However, the frequency range of the visible light spectrum is greater. The visible light spectrum is part of the electromagnetic spectrum that stretches from approximately 400 Terahertz to 790 Terahertz. RF on the other hand only covers 20 kilohertz to 3 Terahertz, indicating that there is close to 130 times more bandwidth in the visible light spectrum than in the RF spectrum. Additionally, no licence is needed to transmit data in the visible light domain, whereas for most RF frequency bands, transmitting licenses are needed. The visible light spectrum has previously been leveraged for communication purposes, most notably with the invention of the photophone by Alexander Graham Bell at the end of the 19th century. The photophone transmitted voice messages over extended distances using sunlight[2]. Researchers even recognised the photophone as a basis for optical fibre communication, a widely used technology today[18].

Building on this legacy, any form of communication for which the visible light spectrum is exploited to convey information, is known as Visible Light Communication (VLC). Within the VLC domain, data can be encoded in a plethora

of ways but generally, the encoding comes down to modulating the intensity of a light source such as an LED or a laser. The information carried by these fluctuations can be detected by a receiver, such as a photodiode or a camera, to extract the original data. The method by which the data is encoded varies with the encoding scheme. In the case of Bell's photophone, the intensity of a reflected beam of sunlight was used to encode audio information[2].

A common approach to VLC is to directly control the intensity of light by, for example, turning it off or on. This is referred to as Active VLC as the light source is actively altered to modulate the signal. A downside to this approach is that a substantial part of the total energy consumption of the system is used to power the light. On the contrary, Passive VLC does not require an actively controlled light source to transmit data. Instead, it relies on ambient light sources, such as sunlight or ceiling lights, to carry information. This greatly reduces the power needed to transfer data for a Passive VLC system compared to an Active VLC system.

Passive VLC has one significant drawback, which is the limited switching speed of modulation devices leading to a reduced throughput. Chapter 2 will further elaborate on this problem. Furthermore, returning to the radio analogy, radios can increase their total throughput by separating all data over multiple channels. For instance, changing the frequency of a radio will result in tuning into another channel. Reflecting back to a VLC system, channels cannot be switched by changing the frequency. The electrical components that the transmitter and radio use to tune into a specific frequency can not handle the high frequencies of the visible light spectrum. However, in the case of visible light, colour filters could be used to divide the spectrum of the source into distinct bands that have limited overlap. These distinct bands could be used to create multiple independent data channels and thus increase the total throughput. An independent colour channel can be achieved by applying a filter to a receiver that corresponds with the band of the chosen channel. This method effectively mitigates the limited switching speed of modulation devices in Passive VLC, thereby addressing the reduced throughput issue. Research into separating the spectrum into different bands was mainly performed for Active VLC but is a novelty for Passive VLC systems. In prior research, mainly high-quality optical films or glass filters[11] are used. Even though these filters are well-characterised and are excellent at admitting a specific band, they are relatively expensive which does not make these filters accessible[21, 15]. Lower-cost filters do exist but they are generally used for aesthetic rather than optical purposes. Therefore, there is less focus on clearly filtering a specific band.

Moreover, when expanding the number of channels, the computational intensity of the decoder increases. As every channel sends independent data, the number of channels is directly tied to the number of computations that have to be done to decode all data. As solely communication is rarely the purpose of any given system, it is crucial to keep overhead in decoding data as little as possible. To make expanding to multiple channels as accessible as possible, the other functions of a system should not have to compromise on performance. Hence, the decoding of data should take as little overhead as possible.

Lastly, the accessibility of Passive VLC would be increased when real-time communication is possible. The alternative is to receive data and decode it later offline, however, a delay would be added which is not beneficial for communication. Prompt decoding of data is essential to allow for real-time communication. However, to even allow for communication, a system has to adjust to the environment in which it is transmitting. As ambient light is used, the dynamics of the source and environment cannot be controlled. Given that ambient light fluctuates, a system should be able to adjust to changes in the environment. This property is vital for real-time applications.

With these problems identified, this thesis aims to explore the use of lower-cost colour filters for channel separation to achieve independent simultaneous transmissions. This would allow for higher data rates while benefiting from the energy efficiency inherent to Passive VLC, all while staying as accessible as possible. We aim to do this by answering the following research question:

- Can multi-channel communication in a Passive VLC system be achieved with low-cost colour filters?

Furthermore, to allow for a more accessible environment, we aim to answer the following questions:

- Can the computational overhead of decoding data in a Passive VLC system be reduced to allow for more efficient scaling with channels?
- Can a Passive VLC platform be provided to allow real-time communication in varying ambient conditions?

1.1 Contributions

This thesis presents the following contributions:

1. In chapter 3, low-cost filters are profiled with the aim of separating incoming lights into multiple channels. The analysis will cover the challenges and shortcomings of cost-effective filters compared to expensive optical filters
2. After characterising the filters, we present a mathematical model to deal with their shortcomings in chapter 4. Enabling multi-channel communication with overlapping filters.
3. To reduce the overhead of the decoding process, An algorithm is proposed in chapter 5. The presented algorithm drastically reduces the number of computations needed to decode the data.
4. Finally, a platform is presented in chapter 6 that implements all the contributions into one platform. The platform can dynamically adjust to the environment to achieve real-time multi-channel communication using cost-effective colour filters.

The contributions are schematically represented in figure 1.1.

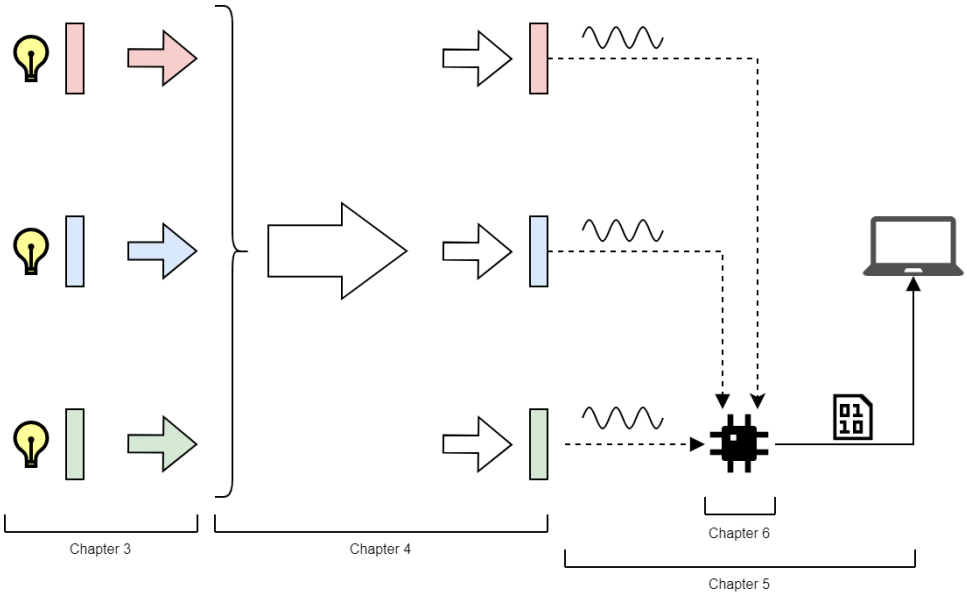

Figure 1.1: **Schematic overview of contributions and their dedicated chapters**

Chapter 2

Background and current work

2.1 Modulation of ambient light

An inherent property of light is polarisation. An electromagnetic wave, such as visible light, consists of an alternating magnetic field and an alternating electric field. These are both perpendicular to each other and the propagation direction. By convention, the angle of the electric field determines the polarisation of light. Polarising filters can exploit this property.

Polarising filters are optical devices that selectively transmit polarised light waves in a specific orientation. Malus' law can describe the degree to which it blocks light. Malus' law states that the intensity of polarised light transmitted through a polariser is proportional to the square of the cosine of the angle between the polarisation direction of the incident light and the axis of the polariser.

$$I = I_0 \cos\theta^2 \tag{2.1}$$

Following this law, controlling the polarisation angle with respect to a fixed polarisation filter would, in turn, control the intensity of the outgoing light. As mentioned, changing the intensity is the key to modulating data in a Passive VLC system. Changing the intensity is achieved using a liquid crystal and a combination of polarising filters.

Liquid Crystals (LCs) are optical devices that are able to change the polarisation of incoming light. LCs have two states that can be reached by applying different voltages. In the unpowered state, the LC changes the polarisation of incoming light by 90°. While in the powered state, it leaves the light's polarisation unaffected. Normally, following Malus' Law, stacking two polarising filters that are 90°out of phase on top of each other, would result in no light passing through. However, by inserting an LC between these filters, the combination would allow for controlling the intensity of outgoing light by switching between the states of the LC. For the powered state of the LC, the polarisation of the light is left unaffected. This will result in the same phase shift of 90°and thus all light will be blocked. However, for the unpowered state, the LC will induce an

additional 90°shift in the polarisation. Following Malus law', the Intensity will not change and thus all light is let through. By using this setup, the intensity of outgoing light can be altered and thus data can be encoded. This process is depicted in figure 2.1.

However, one downside of LCs is their relatively slow switching speeds. Whereas active sources allow for significant bandwidths and can thus achieve remarkable throughputs, LCs have limited bandwidth due to their slow switching speeds. Therefore, the single-channel speeds achieved with LCs in the Passive VLC domain are significantly lower than their active counterparts. Section 2.2 will go into more detail about this topic.

Moreover, the slow switching speed also has a negative side effect. If the LC is continuously switching at sufficiently high driving frequencies, the LC does not have enough time to settle in one state[26]. Before the LC completes the transition from one state the another, the driving signal will already have switched. Consequently, the LC will never reach either of its two states, thereby preventing complete light blocking or complete translucency. This effect is known as saturation and will become more significant for higher driving frequencies. If the driving frequency is too high, no change in the intensity of the outgoing light will be observed. In this case, the LC is *fully saturated*.

Nevertheless, the power draw of a VLC concept with LCs is orders of magnitudes lower than their active counterparts. Generally, power draws in the order of microwatts to milliwatts are achieved for Passive VLC systems[4, 12]. While for Active VLC, generally multiple watts are needed to power a light source[16, 26]. This thesis will use LCs to encode data to achieve Passive VLC.

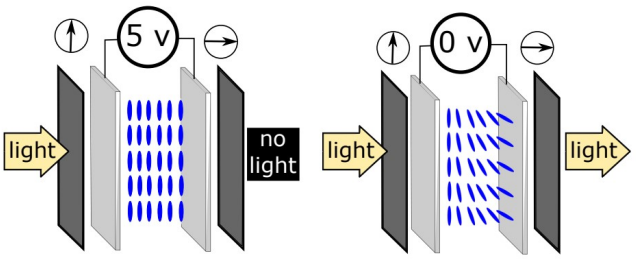

Figure 2.1: **The working principle of an LC, taken from [12]**

2.2 Passive and Active VLC

For all VLC links, a transmitter will direct light towards a receiver with data encoded. Depending on the modulation scheme, data can be decoded by analysing the changes in the light intensity at the receiver. However, the manner in which this change in light intensity is achieved differs between concepts. The VLC domain can is divided into two subdomains: Active VLC and Passive VLC. Active VLC achieves a data link by controlling a light source. Data is modulated by quickly turning a light source on and off. Light sources with high bandwidth can switch on and of fast, therefore high throughputs can be reached. For LEDs

with high bandwidth, speeds in the gigabits per second have been reached for a single channel[23, 9] while for laser communication, ten gigabits per second for a single channel has been reached[17, 13]. This order of magnitude difference is due to their high bandwidth; lasers can switch on and off exceptionally fast. This high bandwidth allows for more advanced encoding schemes and, thus a relatively high throughput.

On the other hand, there is Passive VLC. Passive VLC does not have an active light as a transmitter but rather reuses light that other sources have already emitted. In essence, sunlight or any other form of constant ambient light. As this light cannot be turned on or off, the intensity must be altered in another way to modulate data.

In related work, this modulating is mainly done with a Liquid Crystal(LC) or mirrors. Mirrors can change the reflection angle of incoming light. The mirrors can reflect light towards or away from a receiver and use this change in intensity at the receiver to encode data. Mirrors are the main working principle in [19, 25, 3].

As discussed in section 2.1, LCs have the ability to change their transparency by adjusting the applied voltage. However, not all related works that use LCs to encode data make use of this specific property of LCs. Section 2.6 will provide a more detailed analysis of these related works and how their data is encoded. Nevertheless, what these works have in common is that the throughput of these systems is significantly lower compared to their active counterparts. While Active VLC systems achieve speeds exceeding gigabits per second, passive systems only attain speeds in the range of kilobits per second (see table 2.1). In an effort to enhance throughput and establish Passive VLC as a viable alternative to current wireless communication technologies, this thesis builds upon the foundation of Passive VLC with of LCs.

2.3 Colour filters

The term visible light encapsulates the full spectrum of colours. As mentioned previously, the spectrum for visible light is relatively large, and every part of the spectrum has its own colour. Perceiving all colours together will appear white to the human eye. A colour filter is an optical device that will only let a certain part of the spectrum through while blocking the rest. One downside of using colour filters is that they block a considerable amount of the total energy. The blocking of a specific part of the spectrum is one of the main working principles but all the energy captured in the blocked band is lost.

This thesis aims to analyse the possibility of creating separate channels in the visual light spectrum with by using of colour filters. The novel approach of this thesis aims to achieve this separation in a cost-effective manner, thereby enhancing accessibility and simplifying implementation.

2.4 Modulation schemes

There are multiple ways to encode digital data on a VLC channel. Most schemes utilise one (or a combination) of three techniques. Namely, amplitude modulation, frequency modulation and phase modulation.

Starting with Amplitude Modulation (AM), AM determines the encoded data by analysing the magnitude of the signal at a certain time interval. A common example is On-Off Keying (OOK). The signal being present for a certain amount of time encodes a 1, while the signal not being present encodes a 0.

The second technique, Frequency modulation (FM). FM encodes the data by altering the frequency of a signal. Generally, every symbol will get a unique frequency, called the encoding frequency. For example, transmitting frequency f_1 for a certain amount of time encodes a 1 while transmitting frequency f_0 encodes for a 0.

Finally, there is Phase Modulation (PM). PM encodes data by inducing a phase difference of a known signal for a certain time to encode data.

Whenever the signal is not switched rapidly enough for any of these encoding schemes, flickering will occur. Flickering is the phenomenon when the switching of light is not fast enough such that the human eye can see it. Flickering will be apparent for driving frequencies below $300Hz$[4]. Due to this flickering limit and the saturation of an LC as explained in section 2.1, there is only a small range of driving frequencies, or *bandwidth*, where the LC can operate effectively. As described by LuxLink[4], some modulation types need a wide bandwidth, especially AM or PM schemes with abrupt transitions. FM modulation schemes need a lower bandwidth and are thus better suited to encode data for LCs.

Another benefit of FM is resilience to noise. All noise with a frequency that is not an encoding frequency, will not interfere with the signal. Furthermore, for varying the range, the frequency of a signal does not change as a function of the distance between the transmitter and receiver. However, for the amplitude of a signal, it does. Due to these facts combined, this thesis will continue with FM to encode data.

2.5 Real-time

In addressing the throughput limitations of Passive VLC with LCs, various innovative approaches have emerged. One such approach is ChromaLux[12]. While ChromaLux has achieved significant improvements in data rates, surpassing comparable systems like LuxLink[4] by over 10 times, it does not decode data in real-time. With LuxLink, data is decoded in real-time, implying that requested data becomes available at the receiver shortly after transmission. In contrast, ChromaLux requires data to be recorded and decoded offline to retrieve information, rendering it less accessible for widespread implementation. Chromalux will be discussed in more detail in section 2.6.

This thesis aims to establish a platform for multi-channel real-time modular communication, aiming to enhance accessibility and promote widespread implementation.

2.6 Related passive systems

In this section, we will focus on related works that served as an inspiration for this thesis. Primarily the area of Passive VLC is explored.

2.6.1 Retro-VLC and PassiveVLC

Retro-VLC[16] establishes a bi-directional reader-tag based VLC System. The *ViReader* comprises an LED and a photodiode that can be mounted in existing lighting infrastructure. On the contrary, the *ViTag*, roughly the size of a credit card, consists of a photodiode, a retro-reflective fabric, and an LC. Furthermore, the ViTag is completely battery-less and gathers all necessary energy from a solar-panel present on the tag. In the downlink direction, the ViReader modulates information by blinking the LED. Which the ViTag subsequently receives with its photodiode. To answer, the ViTag modulates reflected light back to the ViReader using the retro-reflective fabric and the LC. A schematic representation can be seen in figure 2.2. Retro-VLC is capable of achieving a downlink throughput of 10 kbps and an uplink rate of 0.5 kbps, with a maximum range of 2.4 meters.

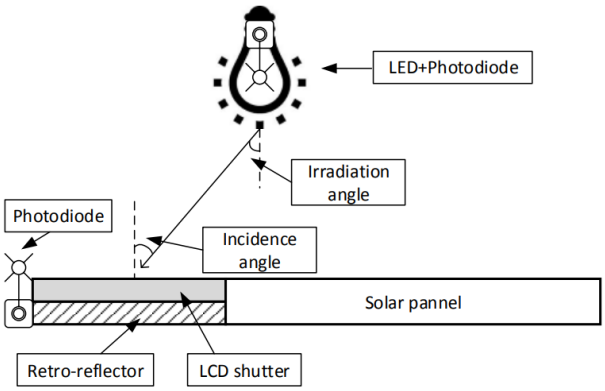

Figure 2.2: **Schematic representation of the Retro-VLC system[16]**

Building upon the Retro-VLC[16] framework, PassiveVLC[26] aims to enhance the uplink data rate. A critical challenge addressed by PassiveVLC involves overcoming the slow switching speed limitation of the LC technology. In the original Retro-VLC system, data encoding had to wait for the LC to fully transition between its states. However, the authors of Passive VLC discovered that during the transition period, the transparency level of the LC undergoes significant changes, providing an opportunity to encode data and effectively boost the system's throughput. With a small range penalty, PassiveVLC can double

the uplink speed to 1 kbps.

Despite the Retro-VLC platform as a whole not being passive, it is important to note that the design of the ViTag component itself follows a passive approach. The ViTag's design, particularly its utilisation of an LC, served as a significant source of inspiration for this thesis. Additionally, the observations made by PassiveVLC regarding the changing transparency level of the LC during its transition phase were instrumental in increasing the throughput of the system discussed in this thesis.

2.6.2 LuxLink and Luxlink+

LuxLink[4] introduces a one-way wireless link that operates solely based on ambient light. Similar to Retro-VLC and Passive VLC, LuxLink utilizes LC technology to modulate data. The system conducted a comprehensive investigation into the limitations of LCs, leading to the adoption of the Binary Frequency Shift Keying (Binary FSK) encoding scheme. In this scheme, the driving frequency of the LC alternates between f_0 and f_1, representing the encoding of 0s and 1s respectively. To decode the data, the receiver applies Fourier analysis to the received signal. LuxLink is capable of achieving a throughput of 80 bps with a maximum range of 65 meters.

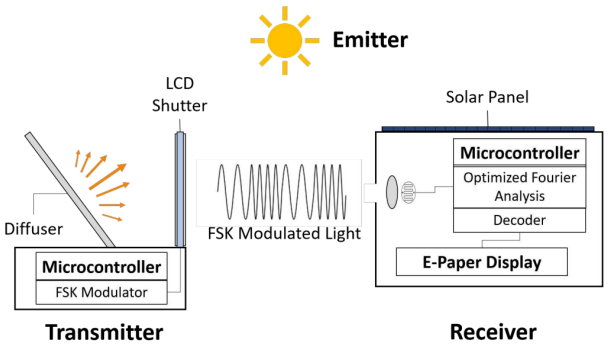

Figure 2.3: **Schematic representation of the LuxLink system[4]**

By closer examining the limitations of LCs for data encoding, LuxLink+[22] aims to improve the throughput of the LuxLink system. This progress is accomplished through the exploration of multiple encoding schemes, each operating within different frequency ranges to drive the LC. These encoding schemes yield higher throughput rates but require a higher signal-to-noise ratio to be decodable. Additionally, LuxLink+ introduces the concept of adaptive link speed, enabling the system to operate at the highest achievable speed based on the prevailing signal-to-noise ratio. Ultimately, LuxLink+ demonstrates the capability to achieve speeds ranging from 80 bps to 1000 bps. However, in order to attain a throughput of 1000 bps, a maximum range of 1.5 meters can be achieved.

This thesis draws significant inspiration from the findings and limitations outlined by LuxLink and LuxLink+ regarding data encoding. In particular, the

encoding scheme used by LuxLink serves as the foundation for the encoding scheme used in this thesis.

2.6.3 PIXEL

PIXEL[27] presents itself as an indoor localisation system that adopts a unique approach to data modulation. Instead of using the intensity of light to encode data, PIXEL utilises colour for information encoding. While the use of different colours for data encoding is not unheard of, PIXEL implements this technique in a manner that remains imperceptible to the human eye. To achieve this, PIXEL incorporates a dispersor at the transmitter, allowing the dispersion of different wavelengths of light into different polarisations. When combined with two polarising filters, it enables the selection of a specific distinct colour. Combining this with an LC, the colour can be changed by changing the state of the LC. By positioning one of the polarising filters in front of the receiver, the light emitted from the dispersor will appear unchanged to the human eye, as it is incapable of perceiving polarisation changes. A schematic representation of PIXEL can be seen in figure 2.4. PIXEL is capable of achieving 14 bits per second up to 10 meters distance.

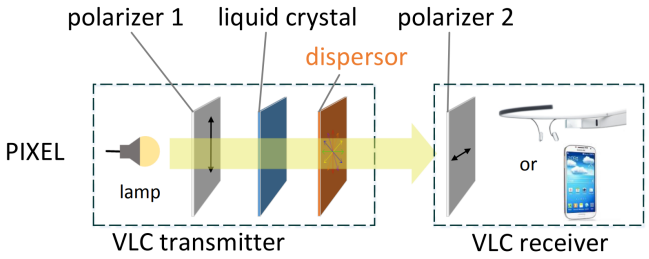

Figure 2.4: **Schematic representation of the PIXEL system[27]**

2.6.4 ChromaLux

ChromaLux[12] is another platform that allows for one way communication using ambient light. Chromalux exploits the birefringence property of LCs to increase contrast when the LC is switching states. When LCs are stacked, a colour shift will occur when changing state(figure 2.5). A colour sensor can be used to measure the change in colour. The relatively rapid change in colour compared to a complete state change of the LCs, allows for earlier detection of state transitions by observing the colour shift. This increased contrast leads to the ability to achieve greater throughputs compared to conventional monochromatic modulation methods. ChromaLux can achieve throughputs of 1 kbps up to a distance of 50 meters

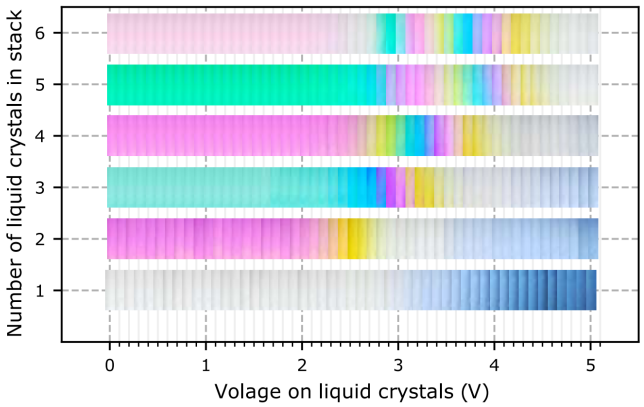

Figure 2.5: **Colour spectrum for a different number of stacked LCs. From [12]**

2.6.5 Summary

Table 2.1 presents an overview of the mentioned related works. It should be noted that this comparison is not an equal comparison, as the approaches and methodologies employed are different between works.

Table 2.1: **Performance comparison of related work**

	Completly passive	Range (meters)	Througput (bps)	Type of modulation	Type of detector
Retro-VLC	No	2.4	10000/500	Intensity	Photodiode
PassiveVLC	No	2	10000/1000	Intensity	Photodiode
LuxLink	Yes	65	80	Intensity	Photodiode
LuxLink+	Yes	1.5	1000	Intensity	Photodiode
PIXEL	Yes	10	14	Polarisation/Colour	Camera
ChromaLux	Yes	50	1000	Colour	Coloursensor

Chapter 3

Splitting Light with Cost-Effective Colour Filters

An option to increase the throughput of a system is to add multiple transmitters along with multiple receivers. This is also referred to as Multiple Input Multiple Output (MIMO). There are multiple ways to ensure that the information in these channels does not interfere with other channels. Where related work often achieves MIMO by exploiting polarisers[1, 20], this thesis aims to use colour filters to create independent channels. Considering the relatively low cost of polarisers, this chapter will investigate the feasibility of using low-cost colour filters as an accessible alternative for channel separation.

The approach for achieving independent channels in the visible light domain using colour filters involves creating channels where specific unique frequencies of light are present. This enables modulation of specific segments within the visual light domain with distinct signals. Consequently, the modulated energy can only traverse through a designated channel and subsequently be received by one corresponding receiver. A typical example is 3D home films. Generally, in cinemas, polarising glasses are used. This way, one eye will only get the adequately polarised image, and applying this to both eyes will give the experience of a 3D image. However, this involves a complex projection setup which is not feasible at home for most people. Therefore home 3D films generally use a technique called anaglyph. Instead of using different polarisations, the images are blue and red-shifted. A particular set of glasses is needed to view the images then. Figures 3.1 and 3.2 show an example of an image that applies anaglyph and the corresponding set of glasses.

Anaglyph uses the fact that red light can only pass through the eye with the corresponding lens in front of it and vice versa. Thus, the data, in this case, an image, can only be received by one eye. If one sees the eye as a receiver of the data, it can be concluded that there are two channels that can only be received by one receiver each. This thesis aims to employ the same principle as anaglyph. For every channel, there will be one transmitter and one receiver

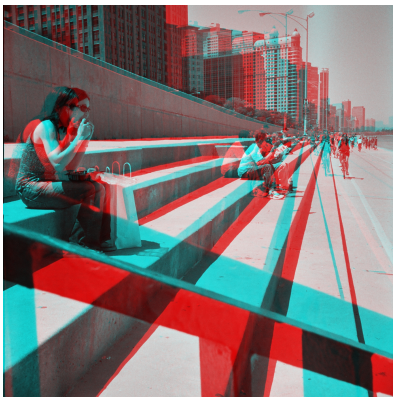

Figure 3.1: **Kim Scarborough, Chicago, IL - Beach Steps (anaglyph)**

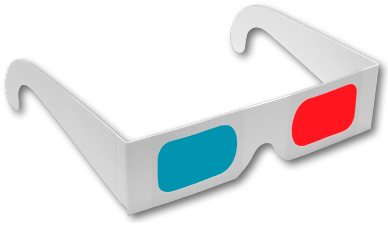

Figure 3.2: **Anaglyph glasses**

with each a filter applied.

In related work, separating channels by wavelength is referred to as Wavelength Division Multiplexing(WDM) or Multi-Colour VLC (VLC-MC)[24, 10, 5, 11]. In case this is achieved by using colour filters, high-quality optical filters are generally used. These filters can capture a specific band of light for various high-end optical applications. They generally come with a well-characterised and narrow response but are relatively expensive. These filters could go up to €100 for the most basic configurations[21, 15]. As the system would need two filters for one channel, it is expensive to scale and increase the number of channels. Therefore, we propose an alternative option. The theatre and photography industry uses film colour filters. These are put over floodlights to produce a coloured light beam for ascetics. This coloured film is around €1 for an A4 sheet in a specific colour [6]. These filters are in the same price range as polarising filters and are therefore relatively accessible. However, as the primary purpose of these filters is to colour a light beam for a visual effect, the spectrum is less important for their purpose. Hence, there is limited knowledge regarding the specific spectral characteristics of the filters. In order to successfully establish channels with minimal overlap, it is crucial to determine which filter captures what specific segments of the spectrum. In the following sections, the filters will be characterised. With these characterisations, tests will be done to evaluate if communication is possible.

3.1 Profiling of spectra

A spectrometer can characterise and collect the spectra of the filters. The filters used[6] are indexed and can be seen in appendix A The setup to determine a spectrum of a filter is relatively simple. A white light was shined on the spectrometer. Between the spectrometer and the light, the desired filter is present. The spectrometer can measure the light passed through this filter and thus derive the spectrum. To understand how much light is blocked and

transmitted by a filter, there has to be a baseline of how much light the source light emits. Determining this baseline is as simple as measuring the spectrum of the light without a filter present. Then, dividing the spectra of a filter by the baseline yields a fraction from 0 to 1 that states how much light the filter lets through. 0 means no light has passed through the filter, while 1 means all light passed through.
All filters have been characterised this way and figure 3.3 shows the results.

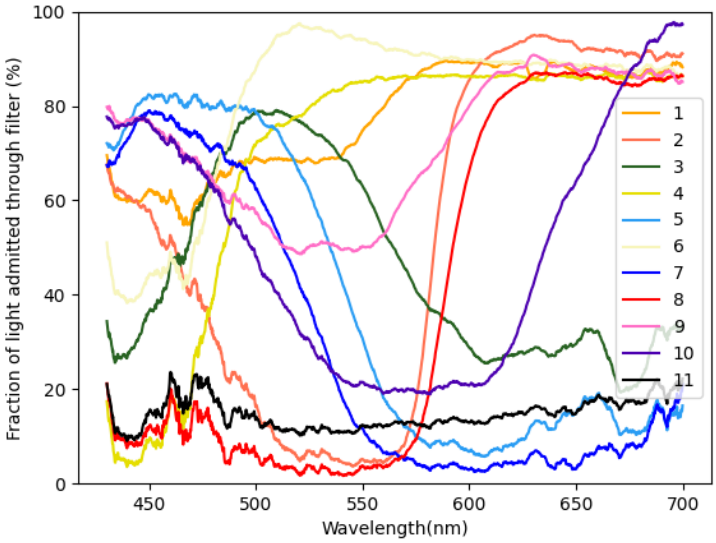

Figure 3.3: **Spectra of all filters, the colours of the lines indicate the approximate colour of the filter**

In the following sections, these spectra will be used to evaluate whether a MIMO approach is viable with cost-effective colour filters.

3.2 Selecting complementary filters

Unlike high-quality optical filters, very few of the filters characterised have a distinct transmission band. It is hard to eliminate all crosstalk. However, minimising it will ensure a better Signal to Noise Ratio (SNR). Filters with minimal crosstalk are called complementary filters. Their spectra overlap as little as possible. As no overlap is impossible to achieve with inexpensive filters, the pair of filters with the smallest overlap was taken. Their spectra can be seen in figure 3.4.
The filters depicted in this figure are filters 7 & 8 from the set. Intuitively, this makes sense as these correspond to blue and red filters respectively. These are on the opposite sides of the visual light spectrum.

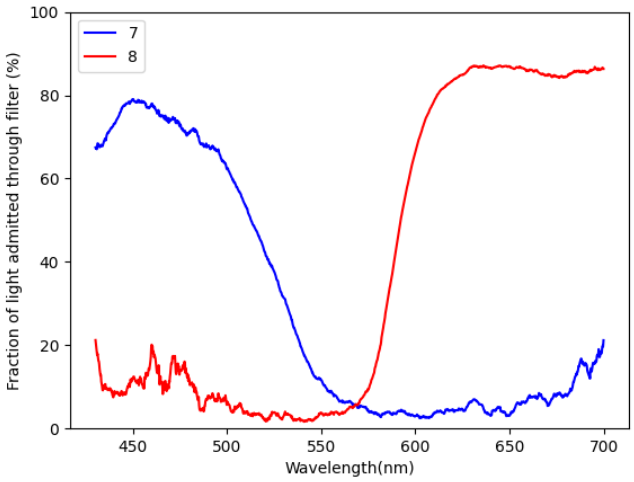

Figure 3.4: **Spectra of blue and red film filters**

3.2.1 Comparing the complementary film filters to the glass filters

As mentioned before, expensive glass filters come with narrower bands. However, in this case, one can argue that that is a disadvantage. Figure 3.5 provides a comparison between optical glass filters and inexpensive filters. The optical filters have narrower bands and less overlap compared to the inexpensive filters. However, as will be elaborated in section 3.2.2, the channels established by the inexpensive filters maintain sufficient independence for effective information decoding. Consequently, the glass filters do not offer any advantage in this scenario. Furthermore, they are more expensive and result in greater energy blockage, yielding a reduced range.

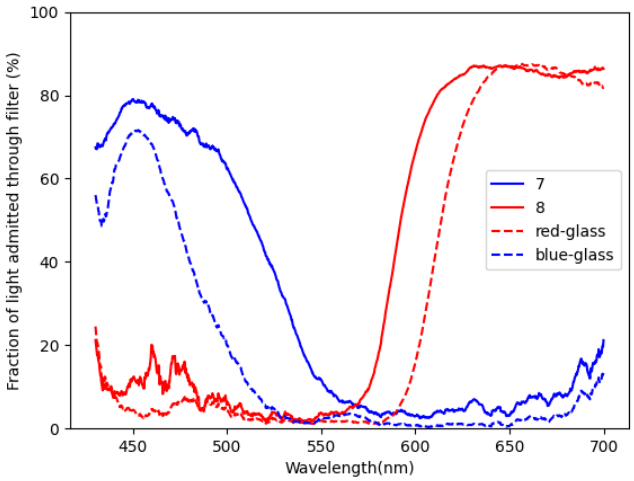

Figure 3.5: **Comparison of spectra of film and glass filters**

3.2.2 Crosstalk evaluation

To verify that the data can be decoded in a system with these two filters, simulations were performed. The purpose of these simulations is to analyse the effect of crosstalk on a channel and whether data can still be appropriately decoded with the amount of crosstalk present. This will be evaluated by comparing the intensity of the desired driving frequency of the LC to the driving frequency induced by LCs of other channels. In addition, the amount of energy that is taken away by a colour filter is characterised. To accurately simulate this, all combinations between filters of the transmitter and receiver have to be tested. For this purpose, a setup is designed to gather the necessary data. Figure 3.6 shows a schematic representation of the test setup. The setup consisted of a transmitter-receiver pair with a couple of items in between.

- Directly after the transmitter, there is an LC.

  The LC can induce a frequency on the channel and thus creating an alternating signal.

- Right after the LC, there is a colour filter.

  This is to set a colour for the channel.

- Finally, there is a colour filter before the receiver.

  The receiver can have one of three configurations.
  1. The same colour filter as after the LC to simulate the desired transfer in a channel.
  2. The complementary filter of the filter after the LC to simulate crosstalk in a channel.
  3. No filter, to set a baseline comparing the other filters too.

In total, gathering all data for one driving frequency involves recording six data sets.
By collecting data for multiple driving frequencies, the crosstalk from one channel to another can be assessed.

In short, the process of evaluating the crosstalk is as follows:

- Data from an experiment where the colour filters of the transmitter and receiver are the same is taken as a baseline.

- Data from an experiment where the colour filter of the transmitter and receiver were complementary and where the frequency was different is added on top of this.

- As the modulation scheme is FSK, the frequencies present in the signal are evaluated to determine whether the desired frequency is still distinct enough.

In addition to evaluating the crosstalk, the effect of a colour filter on the received signal strength is evaluated for multiple frequencies. The effect is determined by comparing the received signal strength with a specific filter in the front receiver to the received signal strength with no filter in the front receiver. It is vital to keep the colour filter at the transmitter and the frequency of the LC the same to get a proper comparison.

Results

First off, the effect of a colour filter on the received signal strength is evaluated. The signal strength is defined as the coefficient of the Fourier transform for the corresponding driving frequency of the LC. As the LC used would saturate at around $1000Hz$, the tests were done with various driving frequencies below $1000Hz$ while staying above the driving frequencies where flickering would occur. The frequencies used were $480Hz$ up until $960Hz$ in steps of $80Hz$.

After analysing the results, it became apparent that frequency has little to no effect on the amount of light passed through a filter. Figure 3.7 shows the results of an experiment with a driving frequency of $640Hz$. The columns are grouped by the colour filter present at the transmitter. The height of the bar represents the ratio between the signal strength of the received signal when using the depicted filter in front of the receiver and the signal strength when no filter is used in front of the receiver. It is clear that a colour filter takes away a considerable amount of light. Even in situations where the filter of the transmitter and the receiver are the same, up to 40% of the energy is lost. Furthermore, the crosstalk between these is significant enough that it cannot be ignored.

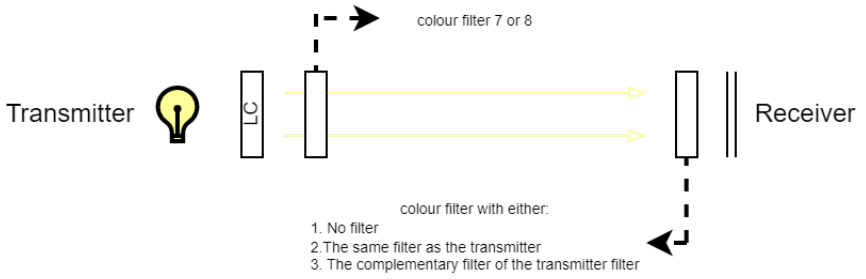

Figure 3.6: **Schematic representation of test-setup to evaluate crosstalk between filters 7 and 8**

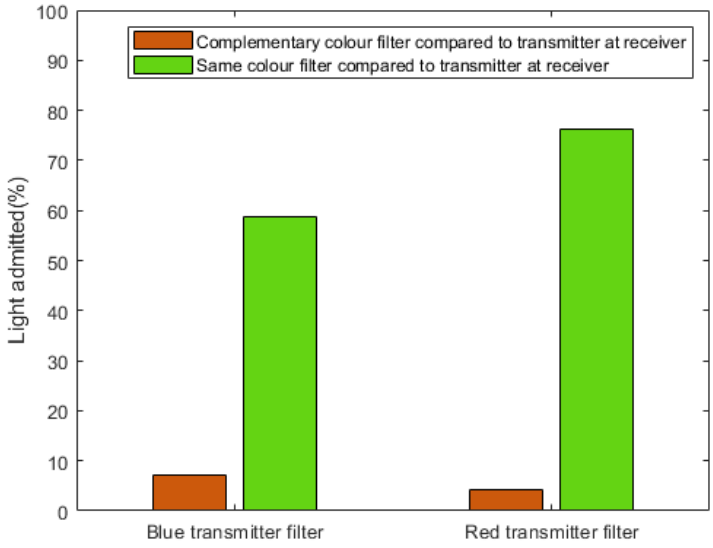

Figure 3.7: **Amount of light received compared to no filter in front of the receiver as a fraction of total light**

After evaluating the effect of a colour filter, the crosstalk was evaluated with all frequency combinations. It is important to recall, the amplitude of the transmitted signal gets smaller with higher frequencies due to the saturation of the LC. Furthermore, deducing from figure 3.7, the most crosstalk will occur from the blue to the red channel. Combining these two filters, the worst situation in terms of crosstalk is from the blue to the red channel, where the blue channel has to lowest available frequency and the red channel has the highest available frequency. Even in this situation, the proper frequencies were still clear enough; thus, the crosstalk was not significant. However, one can also argue that the situation from the red channel to the blue channel is worse. Judging from figure 3.7, the signal-to-crosstalk ratio is worse from red to blue. Nevertheless, also, in this case, the data is still clearly able to be decoded.

Further testing and real-time experiments, together with their results, will be explained in chapter 6

3.3 Trying to increase the number of channels

Naturally, more channels than two are desired to increase the data rate even further. In order to achieve this, there should be a colour filter that spectrum-wise falls in the gap between filters 7 and 8. Looking at the spectra of all filters in figure 3.3, there is no individual filter that meets the criteria. Therefore, the approach of combining filters was tried. The motivation behind this approach is that by stacking filters on top of each other, it may be possible to create a spectrum that fills the gap between the spectra of the blue and red filters with limited overlap. However, looking back at figure 3.7, it can be seen that one filter blocks a significant amount of light. Adding one filter in the path between the transmitter and receiver can take away 40% of the energy. Stacking two filters would only make this number greater. Due to this, stacking filters is far from an ideal situation. Nevertheless, an approach has been tried. All combinations were simulated in software, the combination with filters 3 and 4 fit the gap the best. Figure 3.8 shows the spectra.

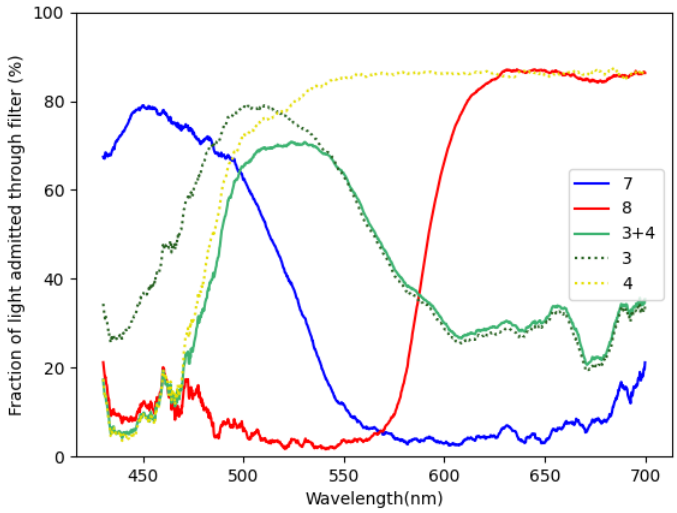

Figure 3.8: **Spectra of the constructed bandpass filter compared to filters 7 and 8**

The figures show a significant overlap with the newly created bandpass filter and the other filters, significantly more than in the two-channel configuration. Furthermore, the total amount of admitted light in the bandpass filter is far lower than the other spectra.
Simulations have been run to see whether independent channels are still viable, which will be presented next.

3.3.1 Crosstalk evaluation

To evaluate the crosstalk of the constructed bandpass filter, a similar simulation like the one in section 3.2.2 was performed with the same setup as shown in figure 3.6. In addition, the frequencies used are the same. The results of this simulation can be seen in figure 3.9. Compared to the previous simulation, there was one key difference, the filter at the receiver was kept constant. The filter at the receiver was the constructed bandpass filter for all experiments. However, the filter at the transmitter was changed between experiments. Therefore, only the crosstalk on the channel with the bandpass filter can be simulated.

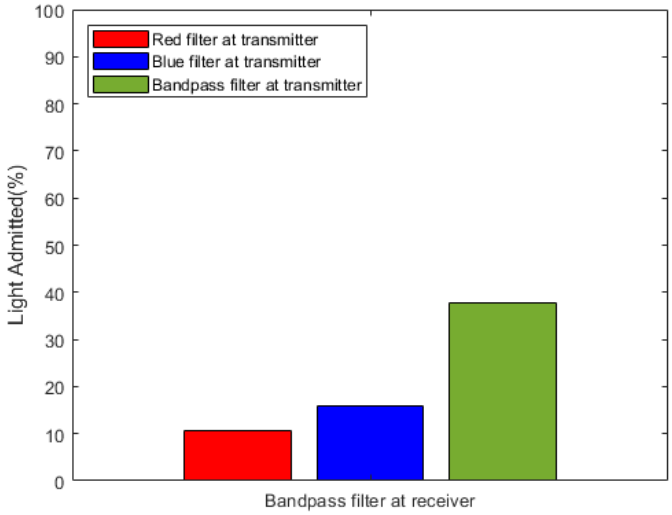

Figure 3.9: **Amount of light received for various transmitter filters with constant bandpass receiver filter as a fraction of total light**

The bars in figure 3.9 represent the amount of light that reached the receiver as a fraction of the light that reached the receiver with no filter present at the transmitter. The key takeaways from figure 3.9 are the following:

- If a bandpass filter is present in the path between the transmitter and receiver, it will take away around 60% of the available energy.
- The crosstalk from the red and blue channels individually is higher than in the two-channel case.

Both points imply that crosstalk will be a greater issue. The crosstalk from the red and blue channels together approaches the signal strength received of the bandpass filter. Combined with the property of the LC that the amplitude decreases for a higher frequency, crosstalk could pose a serious problem.

More simulations were run to investigate the magnitude of this problem. The simulations are similar to those described in section 3.2.2. Signals with different frequencies were superimposed on each other but this time in a three-channel

configuration. The main goal of these simulations is to determine whether these three channels can transmit their own information regardless of what the other channels are doing. As the crosstalk of the red and blue channels to the bandpass channel combined is quite large, there is a concern that it could overpower the signal received on the bandpass channel. This will mainly be the case if the transmitted frequency on the bandpass channel is higher than the transmitted frequencies on the other channels. This exact scenario has been simulated.

After simulations, it became apparent that this issue was significant and could not be solved. Even for small differences in driving frequencies, referred to as the *frequency delta*, where the difference in amplitude is the smallest the system was not deemed stable. When the bandpass channel's frequency exceeded the frequencies of the red and blue channels, the cumulative crosstalk from the red and blue channels began to dominate the signal of the bandpass channel for even the smallest possible frequency delta in the data set. Thus determining the frequency of the bandpass signal is not possible in this case.

After collecting additional data with smaller frequency deltas, it was found that the system stayed completely independent for frequency deltas in the order of $10Hz$. However, this delta was so small that the system was exceptionally error-prone under normal operating conditions and testing showed that the bit error rate would increase. Moreover, achieving the necessary resolution to measure this frequency delta, requires an exceedingly large FFT binsize. However, utilising such a large binsize would significantly impair the system's throughput, almost negating the advantage of having a third channel. The theory for the last claim can be seen in chapter 5. Furthermore, conducting simulations solely with the blue channel and the bandpass channel revealed that if the driving frequency of the bandpass channel exceeds approximately 1.5 times that of the blue channel, the leakage from the blue channel alone becomes sufficient to overpower the signal of the bandpass channel.

In an attempt to mitigate the crosstalk problem of three channels, a concept with static phase shifts between the channels has been simulated. The goal was to see if any static phase offset between channels would improve the frequency delta before overpowering the bandpass signal. If the red and blue channels were completely out of phase, it would improve the situation and move the boundary to around $100Hz$. However, it does not eliminate it. Furthermore, the 1.5 times higher frequency bound between the bandpass and blue channel would remain relatively unaffected. In the end, this was also an unsustainable solution. Combined with the fact that this is just for three channels, adding a fourth channel would be even more complex.

To conclude, trying to create channels by using unique bands is not a viable solution for more than two channels. With the filters used, there is too much leakage between the channels to decode data independently. A potential solution is using some sort of channel estimation to characterise the leakage between the channels and correct for it. This would allow for the use of filters with slightly overlapping spectra. In the next chapter, we propose a channel estimation algorithm to characterise the channels and the crosstalk between them.

Chapter 4

Channel estimation

The last chapter concluded that a channel-wise approach is only possible for filters with little overlap in their admitted spectrum. The crosstalk from the other filters would interfere too much with the signal. Judging from the filter characteristics shown in figure 3.3 and the approaches of combining filters in chapter 3.3, there are not many filter combinations with a unique non-overlapping spectrum. Let alone for more than three channels as tried.
In this chapter, we will propose a way to characterise the leakage between bands and perform a channel estimation to reconstruct the original information. Theoretically, allowing for a great number of channels.

4.1 The model

To determine a way to decode information, a model that represents the setup must be described. Figure 4.1 shows a schematic representation of a two-channel system. The colours do not have to be red and blue, as depicted in the figure. However, both transmitter-receiver pairs should have a colour that is unique to their channel. The arrows in the figure correspond to the coupling from a transmitter to a receiver. The amount of coupling in a transmitter-receiver pair depicts how much energy passes from that transmitter to its corresponding receiver. A coupling factor of 1 states that all energy passes from transmitter to receiver, while a coupling factor of 0 means no energy passes through. In an ideal case, there is a coupling of 1 between a transmitter-receiver pair with the same colour and no coupling between a transmitter-receiver pair with different colours. The coupling between transmitter-receiver pairs that have different colours is also called leakage.

As seen in chapter 3.1, almost all filter pairs have overlapping spectra. This indicates that for most filter combinations, some energy will still be present if a light is passed through both filters sequentially. If energy is still present, it implies there is leakage between a transmitter-receiver pair with different colour filters. If there is too much leakage and no compensation, it could interfere with or even overpower the signal from the transmitter with the same colour filter as the receiver. Defining the coupling between all transmitters and receivers could help characterise the channel and compensate for the leakage between bands.

In the following sections, a mathematical model will be presented that uses these coupling factors to estimate the channels and thus correct for the leakage.

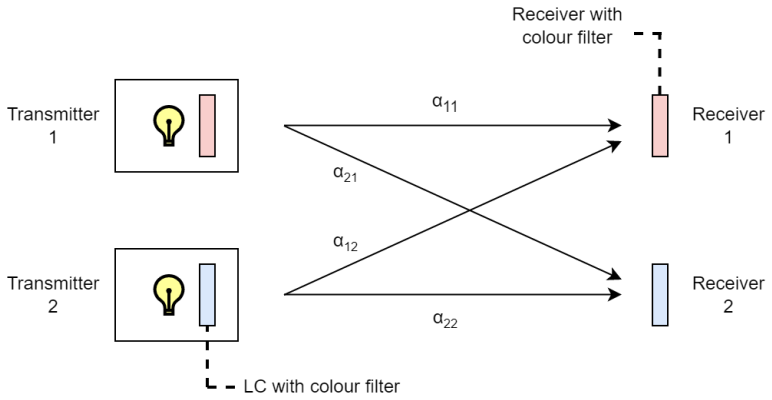

Figure 4.1: **Schematic representation of a system with two channels**

4.1.1 Definition of the parameters

This section will present an overview of all parameters used in the mathematical model of the channel estimation. To provide further clarity on the parameters, figure 4.2 serves as an illustrative example.

Table 4.1: **Table with definitions of general parameters**

Parameter	Description
g_x	Symbol to be encoded for transmitter x.
α_{xy}	Coupling factor from transmitter y to receiver x.
f_g	The frequency to transmit symbol g_x.
S_x	The amplitude of the transmitted signal of transmitter x.
γ	Ratio between the amplitude of two consecutive symbols (due to LC saturation)
c_x	Constant value measured by receiver x due to ambient light.
A	Matrix with coupling coefficient, the definition of the matrix can be seen in section 4.1.2

Table 4.2: **Table with definitions of time domain parameters**

Parameter	Description
$r_x(t)$	The signal received by receiver x in the time domain
$t_x(t)$	The signal transmitted by transmitter x in the time domain
$n_x(g_x, t)$	a function that encapsulates all other harmonics besides the modelled f_g as a function of g_x because the signal transmitted by the transmitter is not a pure sine wave.

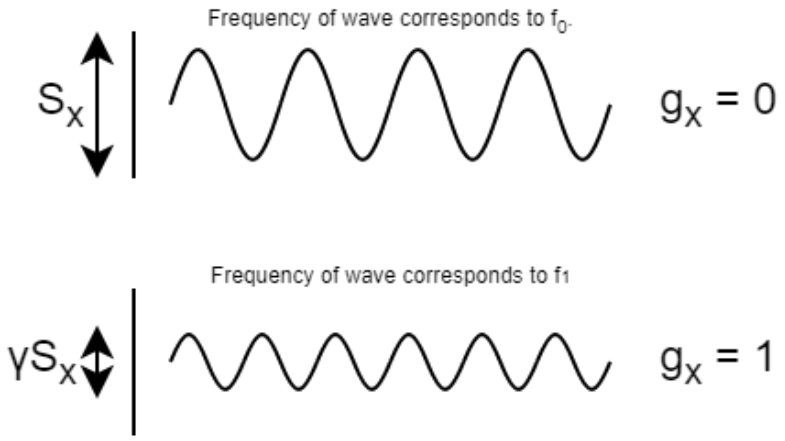

Figure 4.2: **Two signals with their corresponding parameters**

Table 4.3: **Table with definitions of frequency domain parameters**

Parameter	Description
$R_x(f)$	The signal received by receiver x in the frequency domain, $r_x(t)$ in the frequency domain.
$T_x(f)$	The signal transmitted by transmitter x in the frequency domain, $t_x(t)$ in the frequency domain.
$N_x(g_x, f)$	$n_x(g_x, t)$ in the frequency domain.

4.1.2 Estimating the channel

The transmitter

To recall, with FM, the frequency depicts the encoded symbol. Let us consider a system with two transmitters and two receivers as depicted in figure 4.1. Furthermore, considering g_x can only be 0 or 1, the model for the transmitted signal for transmitter one is as follows:

$$t_1(t) = (1 - g_1)(S_1 \cos(2\pi f_0 t)) + g_1 \gamma S_1 \cos(2\pi f_1 t) + n_1(g_1, t) \tag{4.1}$$

Similarly, the model of the transmitted signal for transmitter two can is as follows:

$$t_2(t) = (1 - g_2)(S_2 \cos(2\pi f_0 t)) + g_2 \gamma S_2 \cos(2\pi f_1 t) + n_2(g_2, t) \tag{4.2}$$

A crucial assumption we make is that the frequency components of f_g do not significantly appear in $n_x(g_x)$.

It is trivial to see that the equation simplifies for a value of g_x. For example, choosing $g_1 = 0$ to imply encoding a 0 leads to:

$$t_1(t) = S_1 \cos(2\pi f_0 t) + n_1(0, t) \tag{4.3}$$

Similarly, for choosing $g_1 = 1$:

$$t_1(t) = \gamma S_1 \cos(2\pi f_1 t) + n_1(1, t) \tag{4.4}$$

Thus, the presence of either f_0 or f_1 encodes for a 0 or 1.

The receiver

As explained in section 4.1, leakage occurs from one channel to another. As discussed, a way to model this is with the coupling factor α.
Following the system as depicted by figure 4.1, the general model for the received signal at receiver one can be defined as:

$$r_1(t) = \alpha_{11} t_1(t) + \alpha_{12} t_2(t) + c_1 \tag{4.5}$$

And similarly, for receiver 2:

$$r_2(t) = \alpha_{21} t_1(t) + \alpha_{22} t_2(t) + c_2 \tag{4.6}$$

Noting this down in matrix notation yields the following:

$$\begin{bmatrix} r_1(t) \\ r_2(t) \end{bmatrix} = A \begin{bmatrix} t_1(t) \\ t_2(t) \end{bmatrix} + \begin{bmatrix} c_1 \\ c_2 \end{bmatrix} = \begin{bmatrix} \alpha_{11} & \alpha_{12} \\ \alpha_{21} & \alpha_{22} \end{bmatrix} \begin{bmatrix} t_1(t) \\ t_2(t) \end{bmatrix} + \begin{bmatrix} c_1 \\ c_2 \end{bmatrix} \tag{4.7}$$

The observed signal is $r_x(t)$, though the different $t_x(t)$ signals encode for information. Due to the different couplings between the transmitters and receivers, it is not trivial to decode the information. The original $t_x(t)$ must be constructed to extract the information. Following the described model, the initially transmitted signals can be constructed by inverting the A matrix. However, to do this, all coupling factors have to be known. Section 4.3 explains this process.

Moving to the frequency domain

Equation 4.7 shows a model that can be used to determine $t_x(t)$. However, this model only works for one sample at a time. A set of samples is needed to determine the frequencies present in $t_x(t)$. For FSK, this is ultimately what is important. Furthermore, following equation 4.7, the c_x terms have to be determined to be able to find $t_x(t)$. Following that g_x can only be 0 or 1, the presence of either f_0 or f_1 encodes for a 0 or 1. The Fourier transform determines the presence of these frequencies and thus can directly determine the data in the signal. However, as mentioned before, applying the described matrix transformation for every point collected and then applying one Fourier transform can be quite cumbersome and computationally intensive. Therefore we propose the following approach.
Computing the single-sided Fourier transform for $t_1(t)$ leads to the following.

$$T_1(f) = (1 - g_1) S_1 \delta(f - f_0) + g_1 S_1 \gamma \delta(f - f_1) + N_1(g_1, f) \tag{4.8}$$

Using the linearity property of the Fourier transform and the result of equation 4.5, it is trivial that the Fourier transform of $r_1(t)$ is:

$$R_1(f) = \alpha_{11} T_1(f) + \alpha_{12} T_2(f) + \sqrt{2\pi} c_1 \delta(f) \tag{4.9}$$

And $T_2(f)$ and $R_2(f)$ yield very similar results.

Noting this down in matrix form yields the following equation:

$$\begin{bmatrix} R_1(f) \\ R_2(f) \end{bmatrix} = A \begin{bmatrix} T_1(f) \\ T_2(f) \end{bmatrix} + \begin{bmatrix} \sqrt{2\pi} c_1 \delta(f) \\ \sqrt{2\pi} c_2 \delta(f) \end{bmatrix} \tag{4.10}$$

However, this by itself does not decrease the number of computations. As mentioned, the data is based on the presence of f_0 and f_1. Therefore, information about other frequencies is irrelevant. This implies we can ignore the effect of c_x as it is at $0Hz$. Thus c_x would never influence the f_0 or f_1 frequency bands. Therefore the problem simplifies to the following:

$$\begin{bmatrix} R_1(f_g) \\ R_2(f_g) \end{bmatrix} = A \begin{bmatrix} T_1(f_g) \\ T_2(f_g) \end{bmatrix} \tag{4.11}$$

Noting this down in a singular matrix yields:

$$\begin{bmatrix} R_1(f_0) & R_1(f_1) \\ R_2(f_0) & R_2(f_1) \end{bmatrix} = \begin{bmatrix} \alpha_{11} & \alpha_{12} \\ \alpha_{21} & \alpha_{22} \end{bmatrix} \begin{bmatrix} T_1(f_0) & T_1(f_1) \\ T_2(f_0) & T_2(f_1) \end{bmatrix} \tag{4.12}$$

Extracting the data

As mentioned, the data is encapsulated in the transmitted signal $t_x(t)$ while $r_x(t)$ is the received signal on the receiver side. Following the relation shown in equation 4.12, the equation can be rewritten to:

$$\begin{bmatrix} T_1(f_0) & T_1(f_1) \\ T_2(f_0) & T_2(f_1) \end{bmatrix} = A^{-1} \begin{bmatrix} R_1(f_0) & R_1(f_1) \\ R_2(f_0) & R_2(f_1) \end{bmatrix} \tag{4.13}$$

After computing the results, the data can be decoded by comparing $T_x(f_0)$ to $T_x(f_1)$. If $T_x(f_0)$ is greater than $T_x(f_1)$, channel x encodes for a 0. Otherwise, it will encode for a 1.

Chapter 5 will elaborate how the decoding is exactly done.

4.2 Expanding to more channels

The derived model in 4.1 can easily be expanded to more channels. As an example, adding a third channel will change the model to look as follows:

$$\begin{bmatrix} R_1(f_0) & R_1(f_1) \\ R_2(f_0) & R_2(f_1) \\ R_3(f_0) & R_3(f_1) \end{bmatrix} = \begin{bmatrix} \alpha_{11} & \alpha_{12} & \alpha_{13} \\ \alpha_{21} & \alpha_{22} & \alpha_{23} \\ \alpha_{31} & \alpha_{32} & \alpha_{33} \end{bmatrix} \begin{bmatrix} T_1(f_0) & T_1(f_1) \\ T_2(f_0) & T_2(f_1) \\ T_3(f_0) & T_3(f_1) \end{bmatrix} \tag{4.14}$$

One major downside is that the number of coupling factors scales quadratically with the number of channels. Figure 4.3 shows this in a representation with N channels. Adding a channel will add N more coupling factors from the new transmitter to all receivers. Furthermore, all existing transmitters add a coupling towards the new receiver.

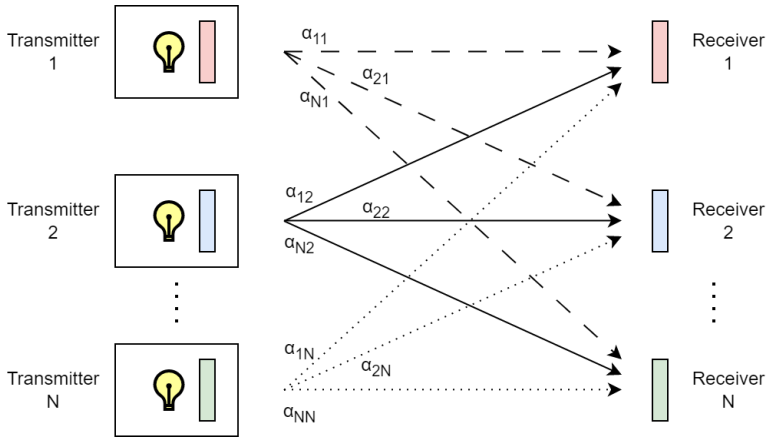

Figure 4.3: **Schematic representation of a system with an arbitrary amount of channels**

4.3 Determining the coupling factors

The coupling factors must be known to construct the $T_x(f_g)signals$. These can be derived manually by performing experiments, but that would compromise on the flexibility of the system. Therefore an algorithm is proposed that can do this automatically. This algorithm consists of a calibration sequence that is predetermined and known to both sides of the link. As both the transmitter and receiver know this information, the coupling factors can be estimated.

Firstly, let us consider a two-channel system again. The calibration sequence consists of channel 1 transmitting a signal with $g_1 = 0$ while channel 2 transmits a signal with $g_2 = 1$. If the light source for both transmitters is similar, $S_1 = S_2 = S$ can be assumed. Following these assumptions and equations 4.1 & 4.2, all $T_x(f_g)$ can be defined as follows:

$$\begin{bmatrix} T_1(f_0) & T_1(f_1) \\ T_2(f_0) & T_2(f_1) \end{bmatrix} = S \begin{bmatrix} 1 & 0 \\ 0 & \gamma \end{bmatrix} \tag{4.15}$$

This allows the receiver to estimate the coupling factors by computing the following equation:

$$A = \begin{bmatrix} \alpha_{11} & \alpha_{12} \\ \alpha_{21} & \alpha_{22} \end{bmatrix} = \frac{S}{\gamma} \begin{bmatrix} R_1(f_0) & R_1(f_1) \\ R_2(f_0) & R_2(f_1) \end{bmatrix} \begin{bmatrix} \gamma & 0 \\ 0 & 1 \end{bmatrix} \tag{4.16}$$

$\frac{S}{\gamma}$ is a quantity that is not known. As this quantity is a scalar and thus will influence every coupling factor equally, it can be set to 1. Section 4.3.2 will explain the legality of this operation.

4.3.1 Expanding to more channels

When expanding this algorithm to more channels, one problem quickly becomes apparent. By looking at equation 4.14, it can be seen that the matrix containing all $T_x(f_g)$ cannot be inverted. Therefore, coupling factors must be estimated in

sets to construct the total matrix from multiple measurements. The matrix can be reconstructed from multiple calibrations with different combinations of two channels. The reconstruction is possible as the coupling factors are independent. One coupling factor only depends on the light transfer from one transmitter to one receiver.

We define the term *calibration step* as the process of performing a calibration with any two channels to construct the full matrix.
A system with three transmitter-receiver pairs needs three calibration steps. Namely channel 1 & channel 2, channel 1 & channel 3 and lastly, channel 2 & channel 3. The coupling factors between two channels are measured in every calibration step, yielding four coupling factors. After all three calibration steps, the following matrices are derived.

$$\begin{bmatrix} \alpha_{11} & \alpha_{12} \\ \alpha_{21} & \alpha_{22} \end{bmatrix}, \begin{bmatrix} \alpha_{11} & \alpha_{13} \\ \alpha_{31} & \alpha_{33} \end{bmatrix}, \begin{bmatrix} \alpha_{22} & \alpha_{23} \\ \alpha_{32} & \alpha_{33} \end{bmatrix} \tag{4.17}$$

The coupling factors that are populating the diagonals show up multiple times. It is likely that they have different magnitudes between the different matrices. Therefore, the columns are scaled such that the diagonals are 1. This preserves the relative ratio between the coupling factors. Section 4.3.2 will explain the legality of this process. Calculating this yields the following matrices:

$$\begin{bmatrix} 1 & \frac{\alpha_{12}}{\alpha_{22}} \\ \frac{\alpha_{21}}{\alpha_{11}} & 1 \end{bmatrix}, \begin{bmatrix} 1 & \frac{\alpha_{13}}{\alpha_{33}} \\ \frac{\alpha_{31}}{\alpha_{11}} & 1 \end{bmatrix}, \begin{bmatrix} 1 & \frac{\alpha_{23}}{\alpha_{33}} \\ \frac{\alpha_{32}}{\alpha_{22}} & 1 \end{bmatrix} \tag{4.18}$$

As all diagonals now have the same magnitude. The final matrix with all the coupling factors can be constructed.

4.3.2 Legality of column-wise scaling

When expanding to more channels in section 4.3.1, the coupling factors were scaled column-wise. This does twist the set meaning of the coupling factors as a coupling factor of 1 does not mean full energy transfer anymore. However, if it does not influence the data, it does not matter in the end.
A key observation in understanding the legality of this operation is that the data decodes by comparing the rows in the matrix with all the $T_x(f_g)$ factors. Let us consider the following matrix with coupling coefficients.

$$A = \begin{bmatrix} W & X \\ Y & Z \end{bmatrix} \tag{4.19}$$

The first column is multiplied by a factor of Γ. Yielding:

$$A = \begin{bmatrix} \Gamma W & X \\ \Gamma Y & Z \end{bmatrix} \tag{4.20}$$

Filling this in to solve for $T_x(f_g)$ yields

$$\begin{bmatrix} T_1(f_0) & T_1(f_1) \\ T_2(f_0) & T_2(f_1) \end{bmatrix} = \frac{1}{\Gamma(WZ - XY)} \begin{bmatrix} Z & -X \\ -\Gamma Y & \Gamma W \end{bmatrix} \begin{bmatrix} R_1(f_0) & R_1(f_1) \\ R_2(f_0) & R_2(f_1) \end{bmatrix} \tag{4.21}$$

$$\begin{bmatrix} T_1(f_0) & T_1(f_1) \\ T_2(f_0) & T_2(f_1) \end{bmatrix} = \frac{1}{\Gamma(WZ - XY)} \begin{bmatrix} ZR_1(f_0) - XR_2(f_0) & ZR_1(f_1) - XR_2(f_1) \\ \Gamma WR_2(f_0) - \Gamma YR_1(f_0) & \Gamma WR_2(f_1) - \Gamma YR_1(f_1) \end{bmatrix}$$

As is apparent in the last derivation, The scaling of the first column with Γ, yields that the second row of the matrix with all $T_x(f_g)$ factors are scaled with Γ. As this maintains the ratio between the two, the data stays preserved. Thus, in this case, column-wise scaling can be done without the loss of data. This is also true for more than two channels.

4.4 Expanding to MFSK schemes

The model has only considered Binary FSK (BPSK). Information is encoded using just two frequencies. However, the model can be expanded to Multiple FSK (MFSK). With this modulation scheme, the amount of bits per symbol is greater than one. Therefore, more encoding frequencies are needed to cover all possibilities. For example, consider a scenario where $T_x(f_2)$ and $T_x(f_3)$ are introduced for a two-channel system such that there are four encoding frequencies. Every encoding frequency would then encode for two bits. With this extension, the model would become:

$$\begin{bmatrix} R_1(f_0) & R_1(f_1) & R_1(f_2) & R_1(f_3) \\ R_2(f_0) & R_2(f_1) & R_2(f_2) & R_2(f_3) \end{bmatrix} = \begin{bmatrix} \alpha_{11} & \alpha_{12} \\ \alpha_{21} & \alpha_{22} \end{bmatrix} \begin{bmatrix} T_1(f_0) & T_1(f_1) & T_1(f_2) & T_1(f_3) \\ T_2(f_0) & T_2(f_1) & T_2(f_2) & T_2(f_3) \end{bmatrix} \tag{4.22}$$

The same relations discussed in the previous sections will still hold. Having more frequencies to play with makes determining the coupling factors easier as one calibration step can determine up to four channels.
In the two-channel example shown in 4.22, the coupling factors can be determined by simply ignoring f_2 and f_3.

4.5 Decreasing the amount of the receivers

The model does not allow for having a lower amount of receivers than the number of transmitters. In this case, it is impossible to solve for the matrix with the $T_x(f_g)$ factors to decode the information. This is because the matrix with the coupling factors can not be inverted as it is not square anymore. Therefore a solution can not be found. Hence this is not a viable solution with the current assumptions.

$$\begin{bmatrix} R_1(f_0) & R_1(f_1) \\ R_2(f_0) & R_2(f_1) \end{bmatrix} = \begin{bmatrix} \alpha_{11} & \alpha_{12} & \alpha_{13} \\ \alpha_{21} & \alpha_{22} & \alpha_{23} \end{bmatrix} \begin{bmatrix} T_1(f_0) & T_1(f_1) \\ T_2(f_0) & T_2(f_1) \\ T_3(f_0) & T_3(f_1) \end{bmatrix} \tag{4.23}$$

4.6 Performance evaluation

Preliminary testing with two and three channels showed that the concept is working. For a detailed review of the test conditions, setup, and result, please refer to section 6.7.

4.7 Recommendations and Future Work

4.7.1 Determining γ

Currently, the amplitude fraction γ is empirically determined. However, γ heavily depends on the relation of the different encoding frequencies and the hardware. If the encoding frequencies change, γ changes. The value must be accurate as γ is critical in determining the coupling factors.
One way to determine γ is by using one transmitter-receiver pair and calculating the ratio of the strengths of the desired frequency components on the fly. This is relatively easy and could be done within the current framework.

4.7.2 Alternate way to determine the coupling factors

The coupling factors play a central role in this model. However, as the number of channels increases, the number of calibration steps required to determine all the coupling factors grows significantly, Therefore, it is desirable to find a new method for determining the coupling factors that exhibits a more linear scaling.

One approach that can be considered involves transmitting an encoding frequency from a single transmitter to all receivers. By analysing the responses of all the receivers, it becomes possible to determine the coupling factors between the transmitter and each corresponding receiver. By implementing this change, the number of calibration steps required to estimate all coupling factors is reduced to just one per channel. As a result, in a 5-channel system, the total number of experiments needed would decrease from 10 to 5.

In matrix notation, it would look as follows:

$$\begin{bmatrix} R_1(f_g) \\ R_2(f_g) \\ R_3(f_g) \\ R_4(f_g) \\ R_5(f_g) \end{bmatrix} = \begin{bmatrix} \alpha_{1x} \\ \alpha_{2x} \\ \alpha_{3x} \\ \alpha_{4x} \\ \alpha_{5x} \end{bmatrix} T_x(f_g) \tag{4.24}$$

This equation can be inverted and the coupling factors could be determined.

An additional aspect is that this process can be performed concurrently for all encoding frequencies. For instance, let's consider a 5-channel system with two encoding frequencies. In matrix notation, it can be represented as follows:

$$\begin{bmatrix} R_1(f_g) & R_1(f_N) \\ R_2(f_g) & R_2(f_N) \\ R_3(f_g) & R_3(f_N) \\ R_4(f_g) & R_4(f_N) \\ R_5(f_g) & R_5(f_N) \end{bmatrix} = \begin{bmatrix} \alpha_{1x} & 0 \\ \alpha_{2x} & 0 \\ \alpha_{3x} & 0 \\ \alpha_{4x} & 0 \\ \alpha_{5x} & 0 \end{bmatrix} T_x(f_g) + \begin{bmatrix} 0 & \alpha_{1y} \\ 0 & \alpha_{2y} \\ 0 & \alpha_{3y} \\ 0 & \alpha_{4y} \\ 0 & \alpha_{5y} \end{bmatrix} T_y(f_N) \tag{4.25}$$

With this addition, the number of calibration steps required could further drop to only 3.

The stability and validity of the models presented in this section are yet to be tested and currently serve as proof of concept. This alternative method of

determining the coupling factors was not further explored as it does not involve a different number of calibration steps for two or three-channel systems, which were the primary focus of the testing conducted.

Chapter 5

Efficient FFT Decoding

In real-world applications, communication is rarely the only purpose of a system. More often, it is a way to gather data that has to be processed further. Therefore the computational time that the system takes up by communicating must be as little as possible.

In the proposed system, the receiver polls the light intensity of multiple channels, proceeds to estimate the channel and then extracts data from the resulting signals. After performing channel estimation, the system must execute the same process for each channel in order to extract the data. With an increasing amount of channels, the system spends more time extracting the data, consequently reducing the amount of available time for other matters.

In this section, we propose an algorithm that dramatically decreases the number of computations needed compared to state-of-the-art Passive VLC systems.

Overview

In the context of non-clocked communication, such as in the proposed system, clock drift emerges as a significant challenge. Clock drift arises from slight deviations in the timing circuits of the transmitter and receiver, leading to differences in their clock frequencies. The issue of clock drift also posed a considerable obstacle for LuxLink[4], as the accumulated disparity over time resulted in synchronisation loss between the receiver and transmitter. To address this problem, LuxLink devised a strategy of evaluating the signal multiple times per bit. Specifically, LuxLink performed the Fourier transform five times per bit and selected the response with the most distinct characteristics. With this strategy, LuxLink was able to address the clock drift and decode the data.
In comparison to other tasks performed by a system, computing a Fourier transform is a time-consuming process. Moreover, as the number of channels increases, the computational load further multiplies, resulting in significant overhead. To mitigate this issue, we propose an algorithm that achieves data decoding with approximately 1.1 Fourier transforms per transmitted bit (approximately 1.1 times the baudrate). In comparison, the LuxLink used five Fourier transforms per bit. This new algorithm dramatically reduces the computational overhead and improves energy efficiency by minimising the time spent

on computations. Additionally, the system is designed to be easily scalable to accommodate additional channels, aligning with the primary objective of this thesis.

5.1 The algorithm

The proposed algorithm encompasses a set of rules for encoding and evaluating data in order to enhance the efficiency of data transmission between a transmitter and a receiver. By considering factors such as clock drift, the algorithm aims to optimise the link's performance. The next section will delve into the fundamental principles of the algorithm, providing a comprehensive explanation of its functionality and benefits.

5.1.1 Modulation of the signal

The algorithm presented in this chapter builds upon the protocol proposed by LuxLink[4] and LuxLink+[22]. The proposed algorithm outlines a one-way communication method between a transmitter and a receiver, utilising the Frequency Shift Keying (FSK) modulation technique, which is a form of FM. FSK is specifically defined for digital transmissions. In FSK, each binary symbol or bit is associated with a specific encoding frequency. For example, f_0 will encode a 0, while f_1 encodes a 1.

In the proposed system, modulation is achieved by driving an LC with one of the encoding frequencies. This action induces a corresponding change in light intensity at the same frequency as the encoding frequency. At the receiving end, the change in light intensity is measured and used to decode the respective symbol.

Determining the basic parameters

As the proposed system uses FSK, the receiver collects samples and performs a Fourier transform to analyse which encoding frequency, and thus symbol, is transmitted. One important metric for this process is the bin size of the Fourier transform. Essentially, the bin size states how many samples are used to compute the Fourier transform. The bin size influences multiple parameters. Section 5.2 will explain more about this metric.

Another important parameter is the sampling frequency. The sampling frequency dictates how often the received light intensity is polled. The sampling frequency and the binsize together heavily influence the throughput of the system. This relation will be further explored in the next section.

Defining a bitframe

An important term to effectively explain the proposed protocol is the term *bitframe*. A bitframe refers to a collection of sequential samples that matches the length of the bin size used in the Fourier transform. Every symbol of data is encoded as a sequence of bitframes with the same encoding frequency. The number of bitframes that resemble a symbol is fixed between the transmitter

and receiver and cannot be changed during operation.

The sampling frequency directly affects the transmission time of a bitframe and thus consequently the time it takes to transmit a symbol. For example, consider a system with a bin size of 8 samples, a sampling frequency of $8kHz$ and assuming 4 bitframes per bit, the timing of each symbol transmission is determined as follows:

$$8 * 4 = 32 \text{ samples per bit}$$

With the known sampling frequency, the transmission time for one bit can be calculated.

$$\frac{32}{8000} = \frac{1}{250} \text{ second per bit}$$

As a result of this relationship, the transmission time of a symbol should be based on the sampling frequency of the receiver.

Choosing the encoding frequencies

As the proposed system uses FSK, specific frequencies will encode for the different symbols. These *encoding frequencies* have to be selected to comply with the Fourier transform. As the samples are taken in discrete time, the Fourier transform will also yield discrete results.

To ensure a signal-to-noise ratio that is as high as possible, the encoding frequencies must be a multiple of the step size of the Fourier transform, also referred to as the *bin width*. To show the importance of this relation, consider the following example in figure 5.1. The example considers a system with specific parameters, a FFT bin size of 50 and a sampling frequency of $5kHz$. The example showcases different pure sine waves with altering frequencies. The plots on the left side represent the signals in the time domain and the right side illustrates the corresponding frequency domain. The frequency domain plots of the first two signal plots show one solitary column at the desired frequency. However, in the third row, this is not the case.

The reason for this deviation is that the frequency of the first two sine waves is multiple of the bin width while for the third signal, it is not. Following the theory of the Fourier transform in discrete time, the bin width of this system is $\frac{5000}{50} = 100Hz$. Because the frequency of the third sine wave is not a multiple of this bin width, two bins at the closest multiples of the bin width appear. Both these bins are lower in magnitude than the bins of the signals that are a multiple of the bin width. Furthermore, there are also a lot of smaller bins at all other frequencies. Both of these facts combined lead to a lower order of distinction for the third signal compared to the first two signals.

In addition, the signals shown in figure 5.1 are ideal sine waves and free from noise. It is crucial to acknowledge that these assumptions do not hold in real-world applications. Therefore, to ensure a signal-to-noise ratio that is as high as possible, it is essential to choose a multiple of the bin width.

Table 5.1: **An example of a packet that encapsulates the word 'Cat'. Complete with preamble and sync bits**

0	00010110	1	01000011	0	01100001	0	01110100	1
ASCII SYN			C		a		t	

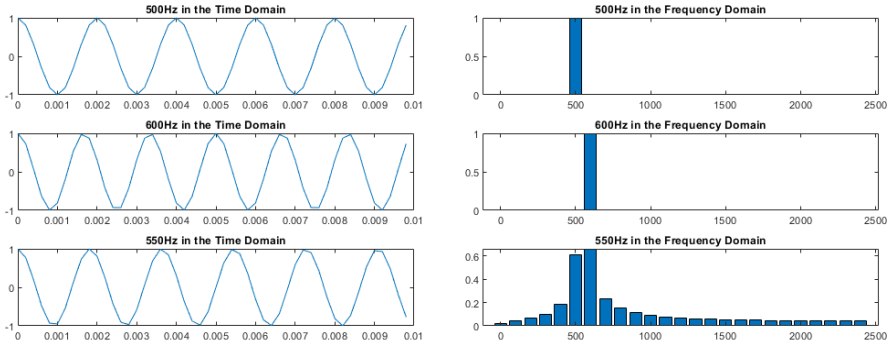

Figure 5.1: **Example of Fourier transform with a binsize of 50 and a sampling frequency of 5kHz**

5.1.2 Towards decoding and syncing

Now that all the important frequencies and terms have been defined, the principles of the system will be explained.

The transmitting part of the system is relatively straightforward. It follows the following steps repeatedly.

1. A data string will be encoded to symbols.
2. The symbols are set in sequence (an example is shown in table 5.1)
3. The data is sent to the receiver.
4. The system will become idle again, waiting for new data.

The receiving side of the system is more complex and uses a more integrated state machine.

At all times, the system is in one of three states, being:

1. No signal
2. Preamble
3. Lock

Initially, the system is in the "no signal" state. In this state, the receiver exclusively applies a Fourier transform to the signal of a single channel for each incoming bitframe.. If any of the encoding frequencies are detected in the bitframe, the system transitions to the *preamble* state. If none of the encoding

frequencies are present, the system proceeds to the next bitframe for the same evaluation.

The purpose of the second state, *preamble* state, is to prevent the receiver from interpreting noise as actual data. Similar to the *no signal* state, only one channel needs to sample during this state. Further details regarding the preamble and its functionality will be provided in section 5.1.3.

If a preamble has been correctly received, the system will switch over to the *lock* state. In the lock state, all channels will be sampled. However, unlike the *no signal* and *preamble* state, not all bitframes will be evaluated. When entering the *lock* state, the first bitframe that comes in will be decoded and it will go through the flowchart as depicted in figure 5.2.

Essentially, the system has to perform two checks to evaluate the validity of the data. Firstly, it detects the presence of an encoding frequency on all channels. If all channels have an encoding frequency present, the system proceeds to check whether the encoding frequencies are distinct enough, which serves as the main synchronisation principle. This synchronisation process will be elaborated on in the upcoming section. If both of these checks pass, the system considers the data as valid. Since a symbol comprises multiple bitframes, the system can wait for the remaining bitframes of the decoded symbol before restarting the loop to decode the next symbol.

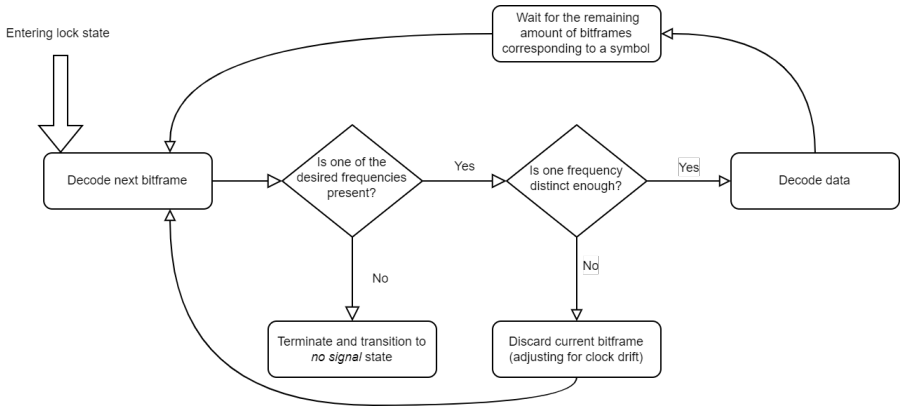

Figure 5.2: **Flowchart of actions in the *lock* state**

Addressing the clock drift

As mentioned at the beginning of this chapter, the clocks of the transmitter and receiver will have a slight difference in their clock speeds. Due to this slight difference in clock speeds between the transmitter and receiver, the bitframes at one side of the link will have a difference in length of time than at the other side of the link. Initially, the bitframes of the transmitter and the receiver start at the same point in time. However, due to the clock drift, the bitframes will start to drift relative to each other This error will accumulate, and in the worst case, this can lead to the situation that is schematically represented in figure 5.3. A

bitframe received by the receiver could receive just as many samples from two different bitframes from the transmitter. In the figure, bitframe M will receive just as many samples from bitframe $N-1$ as it does from N. It is important to note that bitframes $N-1$ and N at the transmitter encode different frequencies, this in turn means that the receiver will receive an equal number of samples of a signal with frequency f_0 as well as f_1 in bitframe M. This makes it as good as guessing which frequency is the right frequency. In the proposed algorithm, the receiver will correct for the drift if it detects that multiple encoding frequencies are present as is the case in biframe M in figure 5.3.

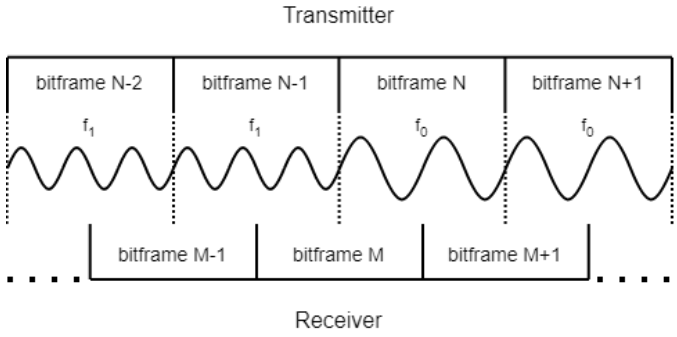

Figure 5.3: **Wost case clock drift**

There are two ways drift can occur.

1. The transmitter is faster than the receiver.

   Bitframes arrive too fast at the receiver; therefore some symbols will be missed.

2. The receiver is faster than the transmitter

   Bitframes arrive too slow at the receiver; the Receiver does not wait long enough and therefore some symbols will be encoded twice.

Correcting for the case where the receiver is faster than the transmitter is relatively easy. It simply involves waiting for a period of time until the next symbol arrives. However, correcting for the situation in which the transmitter is faster than the receiver is more challenging. Compensating for this scenario involves analysing data that has already been sent. Being able to accomplish this requires the system to maintain a certain amount of data in memory, ensuring it is available for future use if necessary. This is a cumbersome task that creates overhead in both a computing-wise and memory-wise sense. Couple this with the fact that this has to be done for every channel and it could quickly lead to much overhead. Besides this, the receiver must also detect which way the drift occurs to correct for drift properly. Which is also a challenging task.

Due to problems adjusting for the clock drift when the transmitter is faster than the receiver, we propose the following solution: the clock of the transmitter is

artificially slowed in a manner that the clock of the transmitter is slower than the clock of the transmitter. In this case, the drift will always flow one way. In the worst-case scenario (figure 5.3), this would translate to the bitframes of the receiver moving to the left compared to the bitframes of the transmitter.

Following the flowchart in figure 5.2, If the worst-case scenario (figure 5.3) occurs, and the algorithm attempts to decode for bitframe M, it will find that the frequency is not distinct enough. In this case, the flowchart states to wait for one bitframe. Since the drift consistently occurs towards the left relative to the transmitter, and considering that a symbol always consists of multiple bitframes, waiting will position the next bitframe (in this case, bitframe $M+1$) at the middle of the symbol. Thus the bitframe will always be encapsulated in a sole encoding frequency. Indicating that data can be properly retrieved.

From empirical testing, a delay between a twentieth to a thirtieth of a bit frame appeared to be a stable optimum between countering any clock drift while not being too aggressive. Being too aggressive will result in the system having to compensate for the clock drift more often than needed and thus efficiency will be lowered. This optimal threshold is highly dependent on the setup of the transmitter and receiver and should be fine-tuned to be as optimal as possible for other setups.

The outlined synchronisation method relies on detecting transitions between two different encoding frequencies. However, for data sequences with consecutive identical symbols, no transitions will occur, leading to the algorithm failing. Section 5.1.4, will discuss how this issue is addressed.

Moving towards fewer bitframes

As mentioned, a symbol is encoded in a sequence of bitframes with the same encoding frequency. A minimum of two bitframes is required to encode a single symbol as this allows for clock drift adjustment. However, there is no additional benefit to having more bitframes beyond this minimum requirement. The time occupied by extra bitframes could instead be utilised to transmit more data, thereby improving the system's throughput.

The only scenario where having more bitframes can be advantageous is at the start of a transmission. After testing it has been observed that the LCs can be slow to react when transitioning from the idle state, potentially resulting in data loss. However, when transmitting a packet, the only moment the LC has to adjust from idle is at the beginning of the packet. Therefore, most systems can run with just two bitframes per bit if an appropriate preamble is in place. The preamble will be further discussed in section 5.1.3.

5.1.3 Preamble

To be more robust and avoid picking up noise as data, every transmission starts should with a preamble. In the proposed algorithm, the preamble consists of one byte that is always the same and only has to be captured by one channel. This byte is $0x16$ in hex and corresponds to SYN in the ASCII standard. The SYN

byte was chosen as it resembles a similar function in the ASCII set and does not encode for a letter or number. Furthermore, the SYN byte only contains one singular sequence of 010 and one sequence of 0110 in its binary notation. This makes it easy for the receiver to sync, as detecting one of these sequences makes it instantly known which part of the preamble is received. Thus, the receiver can automatically deduce when the data starts.

Additionally, as observed in the previous section, LCs need some time to adjust from idle. While the LC adjusts from idle to being driven by an encoding frequency, the transmitted data is generally undetectable for the first few periods of the encoding signal. If the data is undetectable, data loss will occur. How long the adjustment takes depends on the frequency driving the LC. However, from testing, it appeared that sometimes the adjustment takes longer than two bitframes and thus, part of the preamble would be lost. Therefore the first bit of the preamble has double the amount of bitframes. This ensures that, in most cases, the LCs have adjusted by the time the critical parts of the preamble are reached.

An example of a packet including the preamble can be seen in table 5.1.

5.1.4 Sync Bit

In ASCII-based data, most bytes will be letters and numbers. A string of ASCII data converted to binary will generally consist of a mixed sequence of zeroes and ones. Having a mixed sequence of zeroes and ones is desired for the proposed algorithm as it can use the transitions between the different frequencies that encode the zeroes and ones to synchronise again. There is a risk of data loss when data does not contain a lot of these transitions.

A case where this is a concern is when *padding* is used. Padding is the process of adding more bytes that do not have a specific meaning; they are only present to enlarge a packet to comply with the length requirements of the protocol. A well-known protocol which applies this is Ethernet[14]. As these padding bytes do not have any function, they are generally an array of only zeros or ones.

The synchronisation method of the proposed algorithm relies on detecting transitions between two distinct encoding frequencies. However, for padding bytes with consecutive identical symbols, no transitions will occur, leading to the algorithm not being able to synchronisation itself.

As a solution to address the potential issue of consecutive symbols without transitions, we introduce the concept of a sync bit. The sync bit is an additional bit that the transmitter will send after every eight symbols. It is specifically designed to be the complement of the last symbol transmitted. By incorporating the sync bit in this manner, it is guaranteed that at least once every nine symbols, a transition will occur. The choice of one sync bit for every eight symbols was deliberate. For any number of channels, the sync bit aligns with a whole number of bytes, making it easier to encode and decode. A packet with sync bits in place can be seen in table 5.1

5.2 Considerations when choosing a FFT bin size

An important parameter for the proposed algorithm is the binsize of the Fourier transform. In essence, the greater the binsize, the greater the accuracy of the transform, but the longer it takes to evaluate. There are three main effects of increasing the bin size of the Fourier transform. Assuming the sampling frequency will stay the same, these effects will be:

1. The bin width decreases
2. It will take longer to collect the samples.
3. The algorithm itself will take longer to compute

If the bin width decreases, the opposite of these effects will take place.

Increasing the binsize will generate more points in the frequency domain. If the sampling frequency stays the same, there will be more points for the same frequency range. Hence, the bin width will get smaller. Smaller bin widths allow for more flexibility in selecting the encoding frequencies

Second, if the sampling frequency remains constant, the duration needed to gather a complete bitframe will lengthen as the size of the bitframes grows.

Finally, another metric to consider when choosing the binsize is the computational time. The Fourier transform is a relatively computationally intensive algorithm and will take up a significant time of the total overhead caused by the communication system. If the bin size is greater, evaluating all samples will consume more time. Additionally, if more channels are present, more Fourier transforms have to be computed. As a result, the impact of the computational overhead becomes more significant as the number of channels grows.

The computational time required for a fourier Transform is dependent on the hardware used, but in general, it tends to scale beyond a linear relationship. The Cooley-Tukey algorithm[8] is a very efficient algorithm for the Fourier transform. This algorithm uses recursion to achieve a fast and computationally efficient Fourier transform. A downside of the Cooley-Tukey algorithm is that the binsize has to be a power of two. However, this is a relatively small problem as there is flexibility with the sampling frequency. This thesis uses this algorithm to calculate the Fourier transform. The speed benefits outweigh the limitation in available bin sizes

5.3 Results

From testing, the proposed algorithm appeared stable and data could be transferred with high accuracy. Furthermore, the system works for multiple channels. Testing also showed that the system has to compensate for drift for approximately one in ten symbols. This results in 1.1 Fourier transforms to decode one

symbol.

Comparing our approach to Luxlink, we achieve a reduction of almost 80%, which translates to a considerable reduction in computational overhead, especially considering multiple channels. Section 6.7 will give more information about the tests performed, the test setup and in-depth test results.

Chapter 6

Platform design and evaluation

This chapter combines all prior contributions into one platform to enable real-time communication. The transmitter employs multiple channels that use colour filters and the described channel estimation algorithm to achieve independent data channels. With custom electronics, all features are accommodated in a compact package. The following sections go in-depth on the specific parts of the system and present an extensive evaluation. These results show the working of the separate parts of this thesis as well as how all parts of the system work together in various configurations.

6.1 Overview

The objective of the system is to establish a bi-directional communication link. The topology of the communication directions varies. For the *downlink* direction, the system employs the VLC topology discussed in earlier chapters. The transmitter of the downlink can support a configurable number of LCs, corresponding to the desired number of channels. Each LC is associated with a distinct colour filter that represents its channel. On the receiving end of the link, there is an equal number of receivers as the number of channels. Each receiver is equipped with a colour filter that is specific to its corresponding channel. The data intended for transmission is divided among the channels and transmitted according to the format discussed in Chapter 5. Once the transmitted data reaches the receiver, a channel estimation process, as discussed in Chapter 4, will be carried out to retrieve the data.

Separately from the downlink, the platform includes an *uplink*. The uplink could exploit the same topology, but in this case, the system uses a Bluetooth Low Energy (BLE) link for ease of testing and integration. For both the uplink and the downlink, the data transfer is as seamless and effortless for the user as possible. Both sides of the communication link can connect to a phone or PC to send and receive data without any required setup or intervention. This is made possible through the implementation of communication standards that are universally understood by modern devices.

6.2 The photodiodes

The receiver is a microcontroller that uses photodiodes to measure the light intensity of the different channels. The number of total photodiodes in the system equals the number of channels in the system. In order to facilitate proper interfacing between the photodiodes and the microcontroller of the receiver, specific components (as seen in figure 6.1) are introduced between the photodiodes and the receiver. Following the photodiodes, the received signal is amplified by a trans-impedance amplifier. To accommodate variations in the environment and ambient light conditions, a dynamic gain adjustment mechanism has been incorporated. Further details regarding this implementation can be found in section 6.5.

The photodiode circuit generates a voltage ranging from $0V$ to $5V$. However, since most microcontrollers operate at $3.3V$, the voltage needs to be scaled accordingly. To achieve this, a controllable voltage divider was incorporated into the circuit, allowing the maximum voltage to be reduced from $5V$ to $3.3V$. In cases where the signal does not reach the maximum voltage of $5V$ even with the highest gain setting, the scaling can be adjusted to ensure that the measured maximum voltage is scaled to $3.3V$. Further details about the process of adjusting the gain and voltage scaling can be found in section 6.5. Ultimately, the microcontroller will use an analogue-to-digital converter (ADC) to sample the signal, and the software running on the microcontroller will further process the sampled signals.

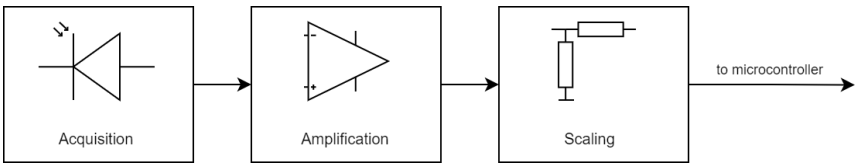

Figure 6.1: **Signal path from the photodiodes to the microcontroller**

6.3 Implementation of the decoding algorithm

In chapter 5, an algorithm was proposed for a computationally efficient approach to decoding an FSK signal. However, the theory mentions frequencies in general rather than distinct values. For the implementation, frequencies have to be chosen that fit the system's physical components. On of the limitations is the saturation frequencies of the LCs. Significant saturation would occur for driving frequencies of $1kHz$. Driving the LCs with higher frequencies would quickly cause them to fully saturate. Therefore, in order to ensure data recovery, it is trivial to keep the encoding frequencies below the saturation limit of the LCs.

In order to select the driving frequencies, the bin size of the Fourier has to be selected. Section 5.2 states the considerations that have to select a proper bin size. Considering that the implemented microcontroller has substantial computational capacities and the capability to sample the photodiodes at a high frequency (as described in section 6.6), it becomes feasible to opt for a rel-

atively large bin width. When the system underwent testing with larger bin widths, occasional instability was observed. This instability presented itself as significant delays in other functions of the system. 64 provided the maximum bin size without encountering the aforementioned instabilities. Therefore, it was selected as the bin size.

Following the theory as defined in chapter 5, the initial choice for the encoding frequencies was $496Hz$ for encoding a 0 and $992Hz$ for encoding a 1. These encoding frequencies were paired with a sampling frequency of $31744Hz$, resulting in the highest possible throughput of 248 bits per second per channel. However, during testing, it became apparent that the system couldn't effectively communicate with these parameters. Based on the Fourier transform theory discussed in chapter 5, the bin width of the system is $496Hz$. With the first bin representing $0Hz$, it can be deduced that the encoding frequencies should align with bins 2 and 3 of the Fourier transform. It appeared with the selected parameters the encoding frequency that corresponds with bin 2 was often mistaken for bin 1 and thus the system would be unable to effectively decode the data. As a result, the parameters were adjusted to yield the highest throughput while not using bin 2 and staying below the $1kHz$ limit. This led to $664Hz$ being chosen as the encoding frequency of a 0 and $996Hz$ being chosen as the encoding frequency of a 1. These encoding frequencies came paired with a sampling frequency of $21248Hz$. These parameters together yield a throughput of 166 bits per second per channel.

6.4 Implementation of the channel estimation protocol

As mentioned in chapter 4, channel estimation is needed for most multi-channel experiments. Since different channel numbers and filter configurations will be tested, automatic channel estimation is necessary. This is achieved during startup through the implementation of a calibration sequence in line with the method as detailed in section 4.3.

Exampled of measured coupling factors are:

$$A_{red,blue} = \begin{bmatrix} 1.00 & 0.05 \\ 0.08 & 1.00 \end{bmatrix}, A_{blue,green} = \begin{bmatrix} 1.00 & 0.45 \\ 0.32 & 1.00 \end{bmatrix} \tag{6.1}$$

The validity of the coupling factors relies on the assumption that the spectrum of the light source remains unchanged. If this assumption does not hold true, the coupling factors may become invalid, necessitating recalibration of the coupling factors.

6.5 Automatic gain control

To account for variations in the environment and source intensity, digital potentiometers can dynamically adjust the gain and scaling of the photodiodes. The ideal gain depends on various factors. Increasing the gain amplifies the signal, but it also amplifies the ambient light (noise). This will translate to a higher

DC bias in the received signal. However, if there is too much ambient light, the receiver could saturate due to the DC bias and no information could be decoded. Since the receiver can monitor the signal from the photodiodes, it can detect the saturation of the signal. Exploiting this, the system can approach the optimal gain using a stepwise process. The process is as follows:

1. The receiver requests for the lowest encoding frequency to be constantly transmitted over the uplink (as for this frequency, the amplitude swing is the biggest)
2. The receiver waits until it detects an oscillation of the desired frequency.
3. The system performs a binary search for the best gain value.

   The condition for increasing or decreasing the gain is whether the ADC has saturated.
4. The receiver indicates that calibration is done.

By default, the scaling is set to reduce the maximum voltage output of the photodiodes from $5V$ to $3.3V$ (refer to section 6.2). However, if during the calibration sequence, it is determined that the gain is at its maximum and the signal has not saturated, the scaling can be adjusted to ensure that the measured maximum voltage is appropriately scaled to $3.3V$. After testing, this appeared to be effective in ensuring the maximum signal-to-noise ratio and allowing for extracting the maximum performance out of the link. Moreover, as the environment is not static, intermediary calibrations are done to ensure the signal will always stay readable.

6.6 The PCB

In order to consolidate all the components and functionalities, a Printed Circuit Board (PCB) was specifically designed to create a streamlined solution. This PCB was designed to be compatible with a microcontroller development board, specifically the Nucleo-144 with an SMT32H7. This choice of microcontroller was made due to its widespread availability at the time of study and its ample computational capabilities, which allowed for extensive experimentation and flexibility in design.

The designed PCB, as shown in figure 6.2, serves as a daughterboard. This integrates seamlessly with the development board. The PCB combines three components essential for the system's operation. Firstly, it incorporates potentiometers that enable precise gain and scaling adjustment for two channels. Additionally, it includes the communication interfaces facilitating the uplink communication. Finally, The PCB design also includes two dedicated interfaces for efficient signal retrieval from the photodiodes.

6.6.1 Debugging connectors

On the PCB, five connectors are arranged in a row. These connectors are not intended for the primary operation of the system, but rather serve for debugging purposes. They allow for the connection of cables to a logic analyzer,

facilitating the analysis of various signals. These signals include internal digital communication signals, potentiometer outputs, as well as signals received from the photodiodes.

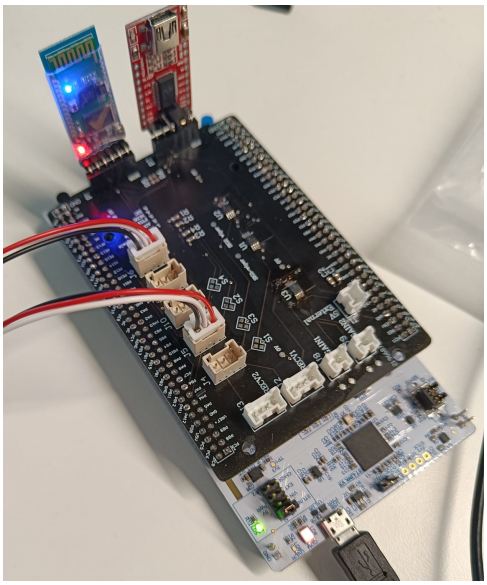

Figure 6.2: **The PCB**

6.7 Results

Throughout this thesis, preliminary testing was conducted to assess the functionality of individual components. However, comprehensive tests that encompass the entire system have not yet been performed. In order to still validate the functionality of the system as a whole, different configurations were tested to evaluate the integration of various system principles. These tests were carried out using custom-developed electronics.

The primary objectives of these tests were to evaluate the following seven questions:

1. Can the data be properly transmitted and decoded with the custom electronics?
2. Does the system properly change the gain with changes in ambient light?
3. What is the range of the system?
4. What is the effect of colour filters on the range?
5. What is the effect of the channel estimation algorithm on the performance of the system?
6. What is the change in performance when using overlapping colour filters?

7. What is the effect of the contents of a packet on the performance of the system?

The tests were conducted in a dynamic office environment characterised by fluctuations in light conditions. These fluctuations were caused by the movements of individuals and changes in natural sunlight. The test environment maintained an average ambient light intensity of 400 lux. The setup accommodated different configurations of channels depending on the specific test being performed. A picture of a test being conducted can be seen in figure 6.3.

Each channel was associated with a unique colour filter, which was applied to an LC component connected to a flashlight. These flashlights emitted light with an intensity of approximately 2000 lux at a distance of 1 meter.

During the tests, the flashlights were directed towards the receiver. The distance between the transmitter and receiver was varied in increments of 0.5 meters, ranging from 0.5 to 7 meters. The performance evaluation at each distance was based on the complete reception of 100 packets, quantified as the Packet Reception Rate (PRR).

In the conducted tests, packets of varying sizes were transmitted, ranging from 5 to 15 bytes for every distance. A portion of these packets encompassed ASCII data, while the remaining packets were exclusively composed of zeroes or ones. This assortment of packet types allowed for a comprehensive assessment of the algorithm's synchronisation capabilities. The different packets were consistently transmitted at intervals of 1 second.

A comprehensive overview of the results, which includes tables displaying the received PRR, are presented in appendix B.

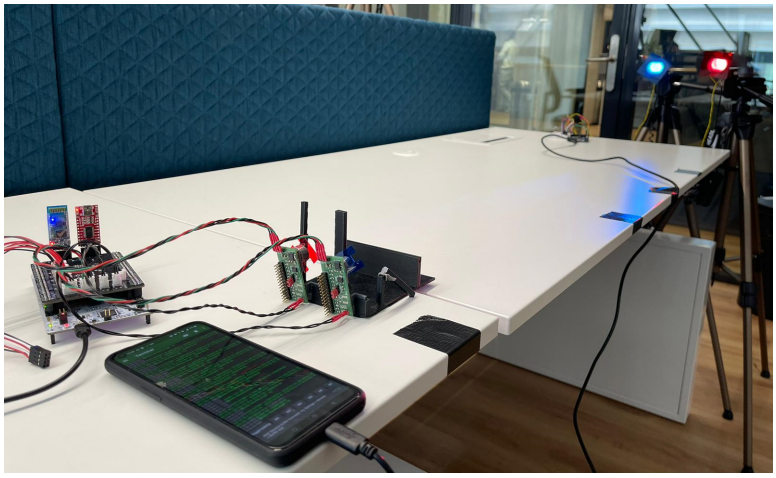

Figure 6.3: **The testsetup used to gather the PRR over various ranges, showing a 2-channel experiment**

6.7.1 1 channel results

In order to assess the system's range and quantify the impact of colour filters on the range, tests were conducted using single-channel setups with various filters. The tests were performed in four different filter configurations, namely:

1. No filter
2. Filter 3, Green (G) filter
3. Filter 7, Blue (B) filter
4. Filter 8, Red (R) filter

The results, presented in figure 6.4, clearly demonstrate a significant decrease in the system's performance when a colour filter is applied. The maximum distance at which the PRR is 100% decreases from 4.5 without a colour filter to 3 meters with a colour filter applied. Moreover, the PRR shows a steeper decline beyond this distance. This reduction in range aligns with expectations, as the application of a colour filter significantly diminishes the energy of the transmitted light.

Among the tested colour filters, filter 3 (G) shows slightly better performance. This can likely be attributed to filter 3 (G) allowing a slightly higher amount of light to pass through. Although the drop from 4.5 to 3 meters is substantial, it is still sufficient to establish a reliable connection between a ceiling light and a device on a desk in most typical scenarios.

The results for the 2-channel tests are depicted in the figure below.

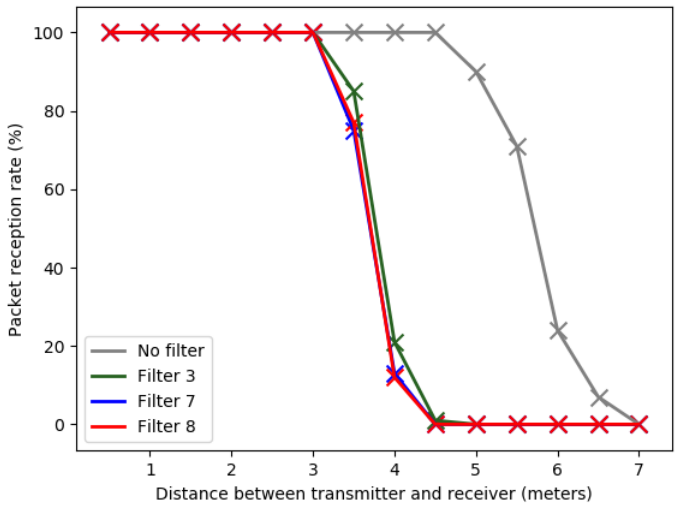

Figure 6.4: **PRR of various 1-channel configurations with varying range**

6.7.2 2 channel results

To evaluate the performance of a 2-channel configuration and the channel estimation, as described in chapter 4, tests were conducted with and without the channel estimation. The four configurations tested are:

1. Filter 7 (B) and 8 (R) without channel estimation
2. Filter 7 (B) and 8 (R) with channel estimation
3. Filter 3 (G) and 7 (B) without channel estimation
4. Filter 3 (G) and 7 (B) with channel estimation

The simulations presented in chapter 3 indicate that a configuration utilising filters 7 (B) and 8 (R) can establish a link without the need for channel estimation, whereas a configuration using filter 7 (B) and the constructed bandpass filter fails to achieve communication. These findings are consistent with the measurement results. Notably, a configuration with filters 3 (G) and 7 (B) cannot achieve communication without channel estimation at any distance. However, in both cases, the application of channel estimation enables successful communication.

The results for the 2-channel tests are depicted in the figure below

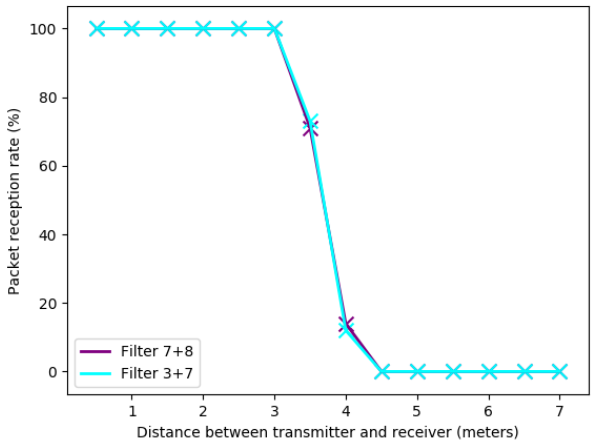

Figure 6.5: **PRR of various 2-channel configurations with channel estimation with varying range**

In conclusion, it can be inferred that the channel estimation algorithm does not introduce any significant penalties. The configuration that operates without the channel estimation algorithm yields results comparable to the same configuration with channel estimation applied. Moreover, these results closely align with their respective counterparts in the one-channel scenario.

6.7.3 3 channel results

Lastly, a three-channel configuration with all three colours was examined. Since the test setup only accommodates two interfaces for connecting photodiodes, an additional external interface was temporarily soldered on the PCB for this specific experiment.

The results for the 3-channel tests are depicted in the figure below

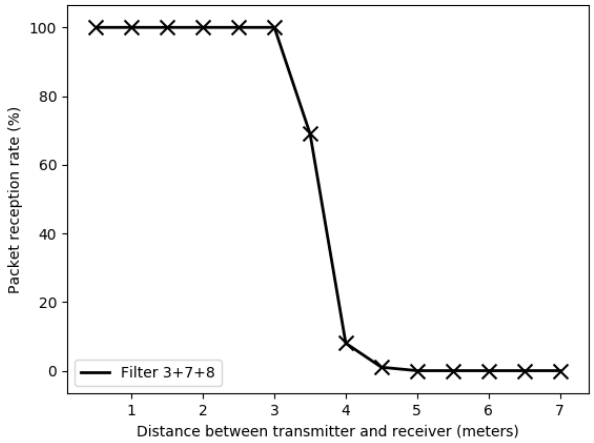

Figure 6.6: **PRR of a 3-channel configuration with varying range**

The three-channel configuration performs similarly to their 2-channel counterparts and thus seemed stable up to 3.5 meters.

6.7.4 The performance of the automatic gain adjustment

As mentioned in section 6.7, the tests were performed in a dynamic office environment with fluctuations in light intensity. However, in all cases, the gain seemed to be correctly adjusted to fit the changing light conditions.

6.7.5 The effect of the packet contents

No significant correlation was observed between the PRR and the content of the packets in any of the experiments. The system exhibited similar performance regardless of whether the packets contained constant content (e.g., all 0s) or alternating content such as ASCII data.

However, the length of the packets exhibited a notable influence on the PRR. In cases where the PRR approached, but did not reach 100%, it was observed that the longest packets experienced a higher likelihood of incomplete reception. An illustrative example is the measurements conducted at a distance of 3.5 meters, where over 80% of the partially received packets exceeded 11 bytes in length. It is worth noting that, in most instances, these packets were only partially received.

6.8 Recommendations

6.8.1 Different microcontroller

The microcontroller chosen for the implementation was the STM32H7. This microcontroller is part of the high-end STM32 family. This microcontroller offers abundant computational capabilities, surpassing the requirements of the application. Its substantial computational headroom proved beneficial during the development and testing of the system. However, it is worth considering more power-efficient and cost-effective alternatives for implementation. Exploring the feasibility of migrating to a microcontroller that strikes a better balance in terms of power efficiency and cost is therefore recommended in future work.

6.8.2 Second bin stability

In section 6.3, it was highlighted that employing an encoding frequency aligned with the second bin of the Fourier transform resulted in unstable outcomes. To unlock potential performance gains, future work could conduct a comprehensive study into the underlying causes of this instability and explore potential solutions. By adhering to the relations of the parameters specified in section 6.3, a substantial 50% increase in throughput could be achieved. This presents a compelling opportunity to enhance system performance and maximise efficiency.

Chapter 7

Conclusion

In this thesis, we aimed to determine if low-cost multi-channel Passive VLC could be achieved by using colour filters. All while staying computationally efficient and accessible for widespread implementation. Based on the findings presented in this thesis, it can be concluded that colour filters are a viable method to create independent channels to transmit any data over a configurable link. Even though the range significantly drops when applying a colour filter, the range will still be significant enough to transmit data from, for example, a light source comparable to a ceiling lamp to a receiver such as a phone or a laptop. However, we also found that due to the poor separation that the low-cost colour filters provide, a channel estimation had to be performed to address the leakage from one channel to another, also referred to as crosstalk. The proposed channel estimation can effectively deal with an overlap in the spectra, allowing for multi-channel communication, even with crosstalk present.

Moreover, significant steps have been made towards energy and computational efficiency in the encoding and decoding processes. This has been achieved by proposing an algorithm that drastically reduces the number of Fourier transforms needed to decode data. Compared to related work, the amount of Fourier transforms dropped by almost 80%, leading to a significantly reduced computational overhead. Furthermore, the decoding also scales to the number of channels in the system which makes widespread implementation of the proposed algorithm for Passive VLC more accessible.

Finally, a PCB was designed to create a compact platform to make these features further accessible for widespread implementation. Additionally, the PCB houses a system to dynamically change the gain of the receivers based on the environment in which the transmission is taking place. This makes it more robust to changes in ambient light.

In conclusion, this thesis has successfully investigated the use of colour filters in achieving low-cost multi-channel Passive VLC while not compromising on computational efficiency or accessibility. The achieved results include a throughput of 166 bits per second per channel, with reliable communication maintained over a range of at least 3 meters.

7.1 Future work

Even though important improvements have been made, there are still some aspects that could be enhanced to improve the working of the designed system. Throughout the thesis, various recommendations have been offered to enhance the system's performance. These recommendations can be summarised as follows:

Determining γ

In the channel estimation, γ is empirically defined. This only works if the delta between encoding frequencies stays constant. However, if the delta changes, γ has to be redefined. Being able to determine these automatically would allow for easier use and implementation. Section 4.7.1 elaborates on this.

Alternate way to determine the coupling factors

In section 4.7.2, an alternative manner of determining the coupling factors was proposed. In future work, the stability and performance of this approach can be investigated. This could drastically reduce the calibration steps needed to determine all coupling factors for configurations with many channels.

Second bin stability

A potential topic that can lead to a high increase in throughput is to investigate if an encoding frequency can use the frequency corresponding to the second bin of the Fourier transform. As mentioned in section 6.3, achieving stability in this aspect would result in a significant boost in throughput, increasing it from 166 bits per second per channel to 248 bits per second per channel in the current situation. This results in an increase of approximately 50%.

Different hardware choice

Currently, the system has been implemented on a high-end microcontroller for ease of testing. However, to increase accessibility, lower cost and lower power would be more beneficial. Section 6.8.1 has provided more information about this topic.

References

[1] S Ammar et al. 'Design and Analysis of LCD-Based Modulator for Passive Sunlight Communications'. In: *IEEE Photonics Journal* 14 (5 2022), pp. 1–17. ISSN: 1943-0655. DOI: 10.1109/JPHOT.2022.3200833.

[2] P. A. Bélanger, D. L. Hutt and K. J. Snell. 'Alexander Graham Bell's Photophone'. In: *Optics and Photonics News, Vol. 4, Issue 6, pp. 20-25* 4 (6 June 1993), pp. 20–25. ISSN: 1541-3721. DOI: 10.1364/OPN.4.6.000020. URL: https://opg.optica.org/abstract.cfm?uri=opn-4-6-20%20https://opg.optica.org/opn/abstract.cfm?uri=opn-4-6-20.

[3] R ; Blokker, T ; Xu and M A Zamalloa. 'Communication with Ambient Light using Digital Micromirror Devices'. 2021.

[4] Rens Bloom, Marco Zúñiga Zamalloa and Chaitra Pai. 'LuxLink: Creating a wireless link from ambient light'. In: *SenSys 2019 - Proceedings of the 17th Conference on Embedded Networked Sensor Systems* (Nov. 2019), pp. 166–178. DOI: 10.1145/3356250.3360021. URL: https://dl.acm.org/doi/10.1145/3356250.3360021.

[5] Hyunchae Chun et al. 'LED based wavelength division multiplexed 10 Gb/s visible light communications'. In: *Journal of Lightwave Technology* 34 (13 July 2016), pp. 3047–3052. ISSN: 07338724. DOI: 10.1109/JLT.2016.2554145.

[6] *Colour filters film 11 colours*. URL: https://www.amazon.nl/gp/product/B0B5Z8XT8P/ref=ppx_yo_dt_b_asin_title_o03_s00?ie=UTF8&psc=1.

[7] Federal Communications Commission. *History of Commercial Radio*. URL: https://www.fcc.gov/media/radio/history-of-commercial-radio.

[8] James W. Cooley and John W. Tukey. 'An algorithm for the machine calculation of complex Fourier series'. In: *Mathematics of Computation* 19 (90 1965), pp. 297–301. ISSN: 0025-5718. DOI: 10.1090/S0025-5718-1965-0178586-1. URL: https://www.ams.org/mcom/1965-19-090/S0025-5718-1965-0178586-1/.

[9] G Cossu et al. '3.4 Gbit/s visible optical wireless transmission based on RGB LED'. In: *Optics Express, Vol. 20, Issue 26, pp. B501-B506* 20 (26 Dec. 2012), B501–B506. ISSN: 1094-4087. DOI: 10.1364/OE.20.00B501. URL: https://opg.optica.org/viewmedia.cfm?uri=oe-20-26-B501&seq=0&html=true%20https://opg.optica.org/abstract.cfm?uri=oe-20-26-B501%20https://opg.optica.org/oe/abstract.cfm?uri=oe-20-26-B501.

[10] Junming Dong, Yanyu Zhang and Yijun Zhu. 'Convex relaxation for illumination control of multi-color multiple-input-multiple-output visible light communications with linear minimum mean square error detection'. In: *Applied Optics* 56 (23 2017), pp. 6587–6595. DOI: 10.1364/AO.56.006587. URL: https://opg.optica.org/ao/abstract.cfm?URI=ao-56-23-6587.

[11] Pengfei Ge et al. 'Optical filter designs for multi-color visible light communication'. In: *IEEE Transactions on Communications* 67 (3 Mar. 2019), pp. 2173–2187. ISSN: 15580857. DOI: 10.1109/TCOMM.2018.2883422.

[12] Seyed Keyarash Ghiasi, Marco A.Zúñiga Zamalloa and Koen Langendoen. 'A principled design for passive light communication'. In: *Proceedings of the Annual International Conference on Mobile Computing and Networking, MOBICOM* (Oct. 2021), pp. 121–133. DOI: 10.1145/3447993.3448629. URL: https://dl.acm.org/doi/10.1145/3447993.3448629.

[13] Ahmed Taha Hussein and Jaafar M.H. Elmirghani. '10 Gbps mobile visible light communication system employing angle diversity, imaging receivers, and relay nodes'. In: *Journal of Optical Communications and Networking* 7 (8 Aug. 2015), pp. 718–735. ISSN: 19430620. DOI: 10.1364/JOCN.7.000718.

[14] 'IEEE Standard for Ethernet'. In: *IEEE Std 802.3-2022 (Revision of IEEE Std 802.3-2018)* (2022), pp. 1–7025. DOI: 10.1109/IEEESTD.2022.9844436.

[15] Thor Labs. *Hard-Coated UV/VIS/NIR Bandpass Filters*. URL: https://www.thorlabs.com/newgrouppage9.cfm?objectgroup_id=1860.

[16] Jiangtao Li et al. 'Retro-VLC: Enabling battery-free duplex visible light communication for mobile and iot applications'. In: *HotMobile 2015 - 16th International Workshop on Mobile Computing Systems and Applications* (Feb. 2015), pp. 21–26. DOI: 10.1145/2699343.2699354. URL: https://dl.acm.org/doi/10.1145/2699343.2699354.

[17] I. Cheng Lu et al. 'Utilization of 1-GHz VCSEL for 11.1-Gbps OFDM VLC Wireless Communication'. In: *IEEE Photonics Journal* 8 (3 June 2016). ISSN: 19430655. DOI: 10.1109/JPHOT.2016.2553839.

[18] Stewart E Miller. 'Lightwaves and Telecommunication: Pulses of light transmitted through glass fibers are lowering costs, increasing speed and capacity, and stimulating new uses of telecommunications systems'. In: *American Scientist* 72 (1 1984), pp. 66–71. ISSN: 00030996. URL: http://www.jstor.org/stable/27852440.

[19] Sifat Ibne Mushfique, Ahmad Alsharoa and Murat Yuksel. 'MirrorVLC: Optimal Mirror Placement for Multielement VLC Networks'. In: *IEEE Transactions on Wireless Communications* 21 (11 Nov. 2022), pp. 10050–10064. ISSN: 15582248. DOI: 10.1109/TWC.2022.3182013.

[20] Asanka Nuwanpriya, Siu Wai Ho and Chung Shue Chen. 'Indoor MIMO Visible Light Communications: Novel Angle Diversity Receivers for Mobile Users'. In: *IEEE Journal on Selected Areas in Communications* 33 (9 Sept. 2015), pp. 1780–1792. ISSN: 07338716. DOI: 10.1109/JSAC.2015.2432514.

[21] Edmund Optics. *Traditional Coated 400 – 699nm Bandpass Interference Filters*. URL: https://www.edmundoptics.com/f/traditional-coated-400-699nm-bandpass-interference-filters/12289/.

[22] Haris Haris Suwignyo. 'Increasing the Performance of Passive Communication with Ambient Light'. TU Delft, Aug. 2019. URL: https://repository.tudelft.nl/islandora/object/uuid%5C%3Ab6637f53-4d37-4e79-a184-240bc2c4f32d.

[23] Dobroslav Tsonev et al. 'A 3-Gb/s single-LED OFDM-based wireless VLC link using a gallium nitride u LED'. In: *IEEE Photonics Technology Letters* 26 (7 Apr. 2014), pp. 637–640. ISSN: 10411135. DOI: 10.1109/LPT.2013.2297621.

[24] Yiguang Wang et al. '4.5-Gb/s RGB-LED based WDM visible light communication system employing CAP modulation and RLS based adaptive equalization'. In: *Optics Express* 23 (10 2015), pp. 13626–13633. DOI: 10.1364/OE.23.013626. URL: https://opg.optica.org/oe/abstract.cfm?URI=oe-23-10-13626.

[25] Talia Xu, Miguel Chávez Tapia and Marco Zúñiga. *Exploiting Digital {Micro-Mirror} Devices for Ambient Light Communication*. 2022, pp. 387–400. ISBN: 978-1-939133-27-4. URL: https://www.usenix.org/conference/nsdi22/presentation/xu-talia.

[26] Xieyang Xu et al. 'PassiveVLC: Enabling practical visible light backscater communication for batery-free IoT applications'. In: *Proceedings of the Annual International Conference on Mobile Computing and Networking, MOBICOM* Part F131210 (Oct. 2017), pp. 180–192. DOI: 10.1145/3117811.3117843. URL: https://dl.acm.org/doi/10.1145/3117811.3117843.

[27] Zhice Yang et al. 'Wearables Can Afford'. In: (May 2015), pp. 317–330. DOI: 10.1145/2742647.2742648. URL: https://dl-acm-org.tudelft.idm.oclc.org/doi/10.1145/2742647.2742648.

Appendix A

Filters Indexes

The filters used are indexed. These indices correspond to the indices shown in various plots throughout the thesis.

Figure A.1: **The eleven filter sheets used throughout the thesis with index**

Table A.1: **The eleven filter sheets used throughout the thesis with written colour**

Index	Colour
1	Orange
2	Rose
3	Green
4	Gold
5	Cyan
6	Yellow
7	Blue
8	Red
9	Pink
10	Purple
11	Black

Appendix B

Testing Results

Tables with the PRR for every experiment at every point tested. If if not explicitly stated, channel estimation was used.

Table B.1: **PRR of various experiments per unit distance**

	Distance (m)													
	0.5	1	1.5	2	2.5	3	3.5	4	4.5	5	5.5	6	6.5	7
1 channel No filter	100	100	100	100	100	100	100	100	100	90	71	24	7	0
1 channel Filter 8	100	100	100	100	100	100	77	12	0	0	0	0	0	0
1 channel Filter 7	100	100	100	100	100	100	75	13	0	0	0	0	0	0
1 channel Filter 3	100	100	100	100	100	100	85	21	1	0	0	0	0	0
2 channel Filter 7 and 8 no channel estimation	100	100	100	100	100	100	70	14	0	0	0	0	0	0
2 channel Filter 7 and 8	100	100	100	100	100	100	71	14	0	0	0	0	0	0
2 channel Filter 3 and 7	100	100	100	100	100	100	73	12	0	0	0	0	0	0
3 channel Filter 3,7, and 8	100	100	100	100	100	100	69	8	1	0	0	0	0	0